REPORT DOCUMENTATION PAGE

Form Approved
OMB No. 0704-0188

PLEASE DO NOT RETURN YOUR FORM TO THE ABOVE ADDRESS.

1. REPORT DATE *(DD-MM-YYYY)*	2. REPORT TYPE	3. DATES COVERED *(From - To)*
2/Jan/2002	DISSERTATION	

4. TITLE AND SUBTITLE
INVESTIGATION OF THE MARCKS-PIP2 INTERACTION THROUGH ELECTRON PARAMAGNETIC RESONANCE SPECTROSCOPY AND THE USE OF A NOVEL SPIN-LABELED PIP2

5a. CONTRACT NUMBER

5b. GRANT NUMBER

5c. PROGRAM ELEMENT NUMBER

6. AUTHOR(S)
CAPT RAUCH MICHELLE E

5d. PROJECT NUMBER

5e. TASK NUMBER

5f. WORK UNIT NUMBER

7. PERFORMING ORGANIZATION NAME(S) AND ADDRESS(ES)
UNIVERSITY OF VIRGINIA

8. PERFORMING ORGANIZATION REPORT NUMBER
CI01-318

9. SPONSORING/MONITORING AGENCY NAME(S) AND ADDRESS(ES)
THE DEPARTMENT OF THE AIR FORCE
AFIT/CIA, BLDG 125
2950 P STREET
WPAFB OH 45433

10. SPONSOR/MONITOR'S ACRONYM(S)

11. SPONSOR/MONITOR'S REPORT NUMBER(S)

12. DISTRIBUTION/AVAILABILITY STATEMENT
Unlimited distribution
In Accordance With AFI 35-205/AFIT Sup 1

DISTRIBUTION STATEMENT A:
Approved for Public Release -
Distribution Unlimited

13. SUPPLEMENTARY NOTES

14. ABSTRACT

20020204 088

15. SUBJECT TERMS

16. SECURITY CLASSIFICATION OF:			17. LIMITATION OF ABSTRACT	18. NUMBER OF PAGES	19a. NAME OF RESPONSIBLE PERSON
a. REPORT	b. ABSTRACT	c. THIS PAGE		105	19b. TELEPHONE NUMBER *(Include area code)*

Investigation of the MARCKS-PIP_2 Interaction through Electron Paramagnetic Resonance Spectroscopy and the Use of a Novel Spin-Labeled PIP_2

Michelle Elizabeth Rauch
Springfield, Virginia

B.A., Bryn Mawr College, 1995

A Dissertation presented to the Graduate Faculty
of the University of Virginia in Candidacy for the Degree of
Doctor of Philosophy

Department of Chemistry

University of Virginia
January 2002

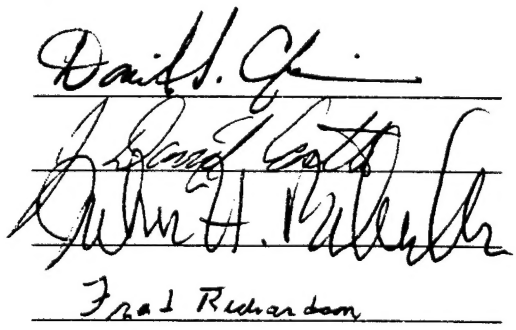

Table of Contents

List of Figures, Tables and Schemes

Abstract

The phospholipid, phosphoinositol 4, 5, bisphosphate (PIP_2) has been implicated in a number of diverse cellular functions, which include membrane trafficking, regulation of the actin cytoskeleton, endocytosis and exocytosis. However, the mechanism for regulation of PIP_2 within the cell during these functions is unknown. One hypothesis for regulation involves controlling the lateral distribution and accessibility of PIP_2 within the membrane, possibly through interactions with proteins or lipid domains.

A spin labeled derivative of PIP_2 (proxyl-PIP_2) was synthesized and characterized through electron paramagnetic resonance (EPR) spectroscopy. The proxyl-PIP_2 is soluble in chloroform and incorporates into lipid vesicles with the proxyl label resting at the membrane interface.

Upon addition of known PIP_2 binding molecules such as neomycin and the PLC δ_1 PH domain, the EPR spectrum of proxyl-PIP_2 shows an increased linewidth, indicative of a decrease in label motion. Furthermore, the proxyl-PIP_2 shows a 1:1 binding upon titration with neomycin, with the same association documented for native PIP_2 affinities. Therefore, the proxyl-PIP_2 can be used as a probe to investigate and quantitate PIP_2 interactions within the membrane bilayer. This probe can also be used to distinguish lateral lipid domains enriched in PIP_2.

MARCKS is a 87 kDalton protein that contains a highly basic region called the effector domain. The effector domain of the protein is the site phosphorylated by PKC, it binds to calmodulin and helps associate MARCKS to the lipid membrane through electrostatic and hydrophobic interactions. MARCKS binds strongly to PIP_2 and may function in a regulatory role by sequestering this lipid. Upon the addition of a peptide

from the MARCKS effector domain the proxyl-PIP_2 EPR spectrum exhibits changes in linewidth due to a decrease in motional averaging, as well as spin-spin interactions resulting from the close proximity of several proxyl-PIP_2. Titration of the MARCKS peptide with lipid vesicles containing proxyl-PIP_2 shows a binding interaction of 2.5-3.5 proxyl-PIP_2 molecules per MARCKS peptide. EPR power saturation of the proxyl-PIP_2 when bound to the MARCKS peptide indicates the label position to be slightly deeper than when not bound to MARCKS. Spin-labeled cysteine derivatives of the MARCKS effector domain show no measurable differences in conformation or position within the bilayer when bound to vesicles containing PIP_2 as opposed to PS as the acidic lipid component. This data is consistent with the hypothesis that the MARCKS protein binds strongly to multiple molecules of PIP_2 in membrane bilayers and regulates their accessibility through non-specific electrostatic interactions.

The views expressed in this article are those of the author and do not reflect the official policy or position of the United States Air Force, Department of Defense, or the U.S. Government

Chapter 1 Introduction into the phosphatidylinositol 4, 5-bisphosphate (PIP_2) and myristoylated alanine rich C kinase substrate (MARCKS) protein interaction

1.1 Phosphatidylinositol 4, 5-bisphosphate (PIP_2)

1.1.1 General characteristics and cellular synthesis

Phosphatidylinositol 4, 5-bisphosphate ($PI4,5P_2$) is a lipid found within eukaryotic plasma membranes. It has been known for quite some time to be the substrate of phospholipase C (PLC) and therefore the precursor to the signaling molecules inositol 1, 4, 5-triphosphate (IP_3) and diacylglycerol (DAG). More recently the importance of $PI4,5P_2$ as a signaling molecule as well as an integral part of several cell processes has placed more focus on $PI4,5P_2$ rather than its products.

Phospholipids are synthesized in both the smooth and rough endoplasmic reticulum in the cell. They are then transferred to the Golgi body where they enter into vesicles and are transferred to various parts of the cell, including the plasma membrane (Mathews and Holde, 1996). $PI4,5P_2$ as well as phosphatidylinositol 3,5-bisphosphate ($PI3,5P_2$) and phosphatidylinositol 3,4,5-triphosphate ($PI3,4,5P_3$) are all derived from phosphatidic acid which is converted to cytidine di-phosphate (CDP)-diacylglycerol (DAG). Upon addition of myo-inositol and catalysis by phosphatidyl-inositol synthase, phosphatidylinositol (PI) is produced. Depending on the pathway and enzymes present, PI can then be converted to either $PI4,5P_2$, $PI3,5P_2$, $PI3,4P_2$ or $PI3,4,5P_3$ (Scheme 1.1-1).

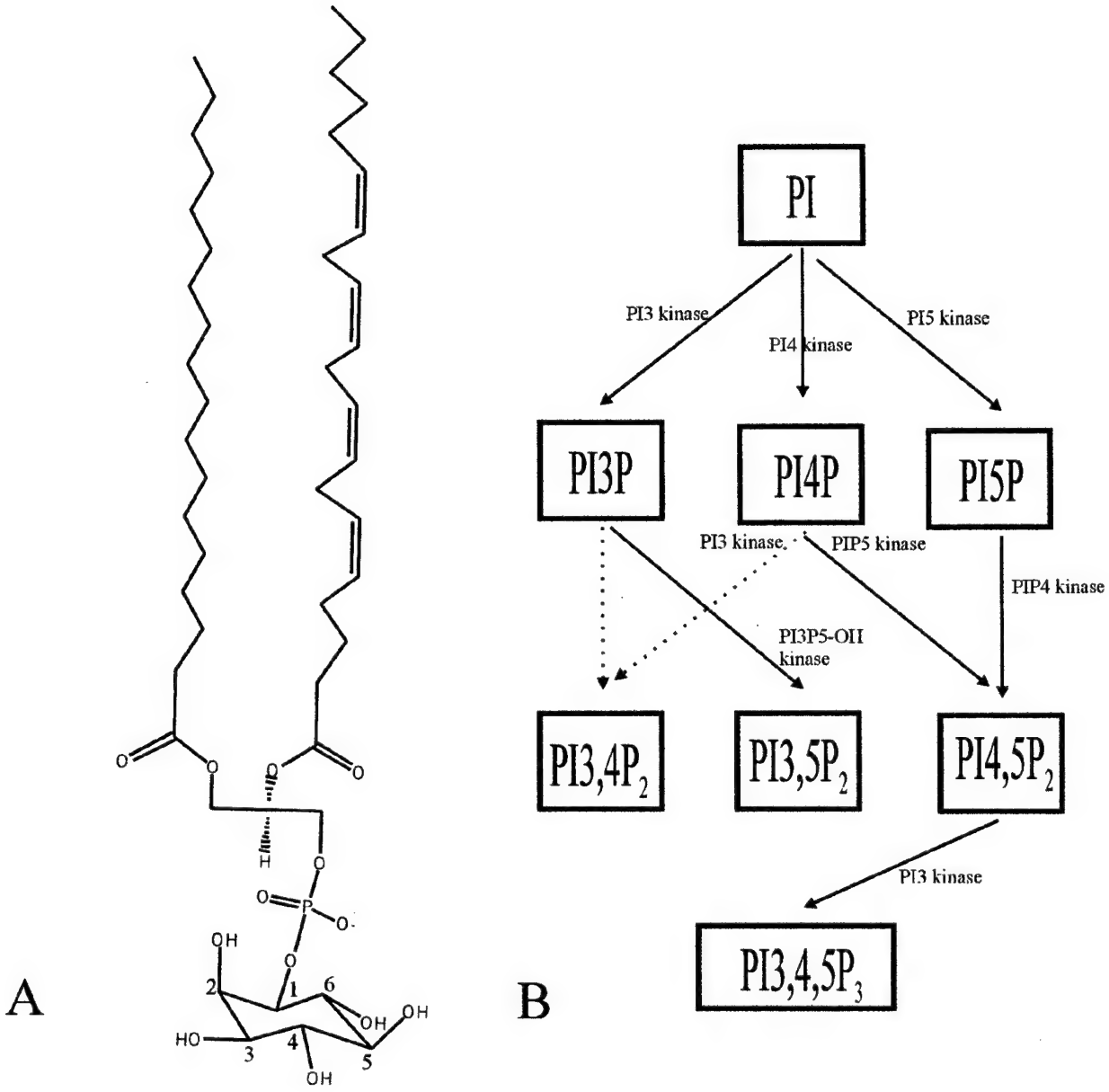

Scheme 1.1-1 A) Structure of phosphatidylinositol, with numbers indicating possible phosphorlation sites on inositol head group. B) Phosphatidylinositol synthesis pathways including well documented enzymes. Pathways indicated with a dashed line are less well defined. (Vanhaesebroek et. al., 2001)

1.1.2 Hydrolysis of PIP_2

All three polyphosphatidylinositols can be synthesized from PI. However, it is $PI4,5P_2$, hereafter abbreviated as PIP_2, with its known role as the precursor to IP_3 and DG, as well as its abundance, that make it the most investigated of the phosphatidylinositol lipids. There are three families of PLC enzymes responsible for the hydrolysis of PIP_2. The three have been termed PLC-β, PLC-γ and PLC-δ (Toker, 1998). The breakdown of PIP_2 by each family of PLC is activated in a slightly different manner. However, the basic principle is the same: there is an activation event, which occurs as the result of G protein activation for PLC-β or receptor tyrosine kinase activation for PLC-γ, and binding of the PLC to PIP_2 with the successive hydrolysis into IP3 and DAG (Toker, 1998). Once broken down from PIP_2, IP_3 is released into the cytosol where it travels to the endoplasmic reticulum and stimulates the release of calcium. Upon calcium release, DAG, which is still within the plasma membrane, binds to protein kinase C (PKC) and increases the enzyme's affinity to calcium. This sequence of events then stimulates PKC to phosphorylate serine and threonine residues on membrane-bound target proteins including the myristoylated alanine rich c-kinase substrate protein (Figure 1.1-1) (Mathews and Holde, 1996).

1.1.3 Additional roles in the cell

In addition to its role as a precursor to IP_3 and DAG, PIP_2 has been found to be involved in the regulation of the actin cytoskeleton, membrane trafficking, endocytosis, and exocytosis (Czech, 2000).

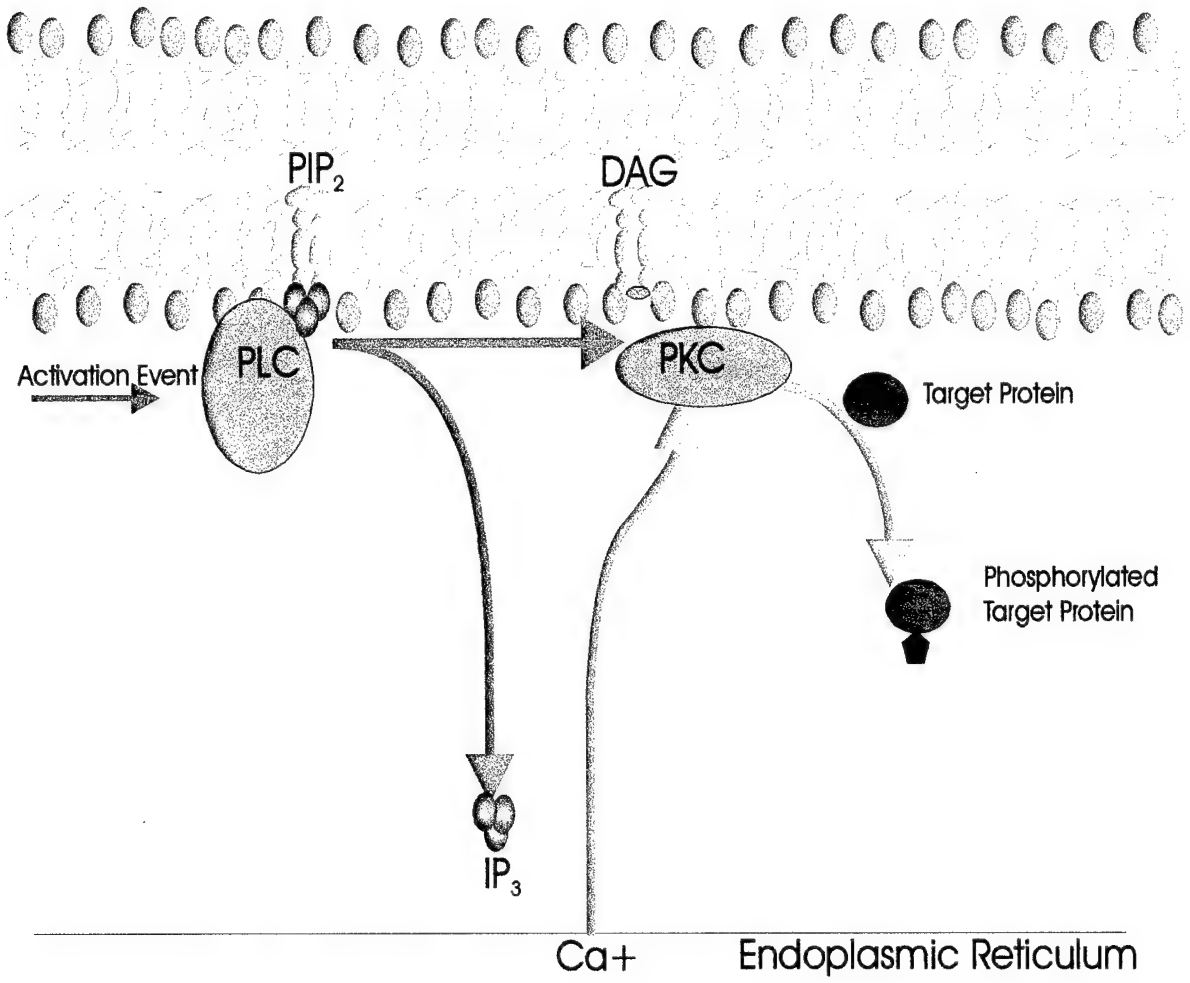

Figure 1.1-1: Breakdown of PIP_2 by PLC into second messengers IP_3 and DAG

It has been found that PIP_2 can bind to actin-capping proteins such as profilin and gelsolin (Toker, 1998). Gelsolin is one of the proteins responsible for cutting actin filaments into two shorter filaments and then capping the barbed ends. This capping inhibits the polymerization of the actin filaments. Once the capping proteins have been removed from the ends of the filaments, the actin filaments can then polymerize. PIP_2 has been found to bind to peptides corresponding to sequences containing basic amino acids from gelsolin. In addition, PIP_2 uncaps F-actin when added to permeabilized platelets. These findings suggest that PIP_2 plays a regulatory role in the uncapping and subsequential polymerization of actin (Toker, 1998).

PIP_2 has been found to act as a cofactor for the membrane associated enzyme phospholipase D (PLD). Adenosine diphosphate ribosylation factors (ARFs) and Rho proteins are small GTPases that regulate phospholipase D and control a variety of other cellular activities including vesicle formation and trafficking as well as the organization and dynamics of the actin cytoskeleton. ARFs are involved in controlling the sequestering of coat proteins to the Golgi membrane while Rho proteins are involved in mediating actin cytoskeletal dynamics that lead to control over cell shape, movement and polarity (Martin, 1997). PIP_2 activates PLD in vitro and has been found to directly interact with ARF1. While not yet fully understood, it is believed that PIP_2 is involved in membrane trafficking through its interaction with these proteins (Martin, 1997; Toker, 1998).

PIP_2 has also been implicated in both endocytosis and exocytosis processes. Dyamin is a GTPase enzyme necessary for the fission of clathrin-coated vesicles originating from

the plasma membrane during endocytosis. Dyamin has been found to be stimulated by and bind preferentially to PIP_2 over $PI3,4,5P_3$. It is hypothesized that PIP_2 localizes dyamin to the plasma membrane and activates its GTPase activity. Other evidence supporting the involvement of PIP_2 in endocytosis is the colocalization of several enzymes known to either synthesize or degrade PIP_2. These enzymes include synaptojanin, a polyphophatidyl 5-phosphatase and phosphatidylinositol 3-kinase which has previously been noted in a later step of endosomal trafficking. Likewise, several enzymes responsible for PIP_2 synthesis are required for exocytosis. Studies have shown that phosphatidyl 5-kinase and phosphatidyl 4-kinase as well as phosphatidylinositol transfer protein but not phosphatidyl 3-kinase are required for the priming necessary for exocytosis. In addition the priming is halted by addition of PLC (Martin, 1997; Toker, 1998).

1.1.4 Two PIP_2 binding molecules: PLC δ_1 PH domain and Neomycin

In many of the roles played by PIP_2 the lipid functions to translocate soluble proteins to the membrane interface. One protein modular domain that has been found to specifically interact with PIP_2 is the pleckstrin homology (PH) domain (Lemmon et al., 1996). The PH domain is named after pleckstrin, a platelet protein that is a PKC substrate. The PH domain consists of approximately 120 amino acids, and has a molecular weight of about 22 kDaltons (Mayer et al., 1993; Hirata et al., 1998). This compact protein module has been found in over a hundred proteins expressed in animals, protista and yeast (Shaw, 1996). A large number of the PH domain containing proteins are involved in intracellular signaling (Lemmon et al., 1999; Ferguson et al., 1994). Both X-ray crystallography and NMR have shown the PH domain to have a distinct

seven-stranded β-sheet sandwich of two orthogonal β-sheets, closed off at one corner by a C-terminal α-helix (Hirata et al., 1998; Lemmon et al., 1999; Gibson et al., 1994).

PH domains have been shown to bind to βγ subunits of G proteins, to WD motifs of protein kinase C, to inositol 1, 4, 5-triphosphate (IP_3) and to PIP_2 (Hirata et al., 1998; Lemmon et al., 1999). Additionally, it is known that the PH domain of phospholipase C-δ_1 (PLC-δ_1) forms a 1:1 high affinity complex with PIP_2 with a K_d of about 1.7 μM (Bucki et al., 2000; Ferguson et al., 1994; Shaw, 1996). It is the first 60 amino acids of the PLC-δ_1 which consists of the N-terminal portion of its PH domain, that competitively binds to PIP_2 and IP_3 (Hirata et al., 1998). The structure of the rat PLC-δ_1 PH domain complexed to IP3 was resolved by Ferguson et al and published in 1995 as seen in Figure 1.1-2. The inclusion of a PH domain in several signaling molecules naturally leads to the hypothesis that PH domains are involved in the signaling process. One proposed physiological role for the PH domain involves targeting the PLC-δ_1 enzyme to the surface of the membrane through binding with PIP_2, thereby allowing catalytic access to the PIP_2 (Hirata et al., 1998; Shaw, 1996).

In addition to binding to proteins and protein modules such as the PH domain, PIP_2 is known to bind to the oxotoxic and nephrotoxic polycationic antibiotic neomycin. Neomycin has six primary amine groups (Figure 1.1-3) and an average charge of +4.5 in 100 mM KCl pH 7.0 (Arbuzova et al., 2000a). Neomycin has been shown to bind in a 1:1 manner with PIP_2 with a binding affinity of about 10^5 M^{-1}. The binding of neomycin to PIP_2 blocks the hydrolysis of the lipid by PLC thereby inhibiting the subsequent production of IP3 and DG (Chauhan, 1990). The well established binding of neomycin to PIP_2 makes it a useful molecule for investigating PIP_2 in membranes. A nice example

A

B

MHGLQDDPDL QALLKGSQLL KVKSSSWRRE RFYKLQEDCK TIWQESRKVM
RSPESQLFSI EDIQEVRMGH RTEGLEKFAR DIPEDRCFSI VFKDQRNTLD
LIAPSPADAQ HQVQGLRKII HHSGSMDQRQ K

Figure 1.1-2: A) Structure of PLC δ_1-PH domain complexed with IP_3 B) Sequence of PLC δ_1 PH domain structure shown (Ferguson et al., 1995)

of this use was documented by Arbuzova et al (2000) through the utilization of three different fluorescently labeled neomycin molecules to probe for PIP_2 in membrane vesicles.

The above discussion has only touched on several of the known PIP_2 interactions. Although, PIP_2 has been found to be involved in many different cell processes, the phospholipid's precise purpose in each scenario is not totally understood. An evolving popular hypothesis is that the localization and lateral domain formation of PIP_2 within the cell membrane allows for the segregation of the many signaling pathways that depend on PIP_2 (Toker, 1998; Raucher et al., 2000; Arbuzova et al., 2000b).

1.2 Myristoylated alanine rich c-kinase substrate protein (MARCKS)

1.2.1 Discovery and characteristics

The discovery of the protein Myristoylated Alanine Rich C Kinase Substrate (MARCKS) was originally documented in 1982 by Wu and associates as a 87kDa protein found within rat brain fractionated nerve endings that acted as a major endogenous substrate for PKC (Arbuzova et al., 1997; Blackshear, 1993; Albert et al., 1986; Yamauchi et al., 1998; Wu et al., 1982). The MARCKS protein was soon isolated in several species including monkey, rat, human and cow (Albert et al., 1986). MARCKS has a molecular weight between 80 and 87 KDaltons depending upon species and has been found in cells in the brain, macrophages, lymphocytes and fibroblasts (Albert et al., 1986; Blackshear, 1993; Taniguchi and Manenti, 1993; Zolessi et al., 1999).

Initially when MARCKS was isolated from rat synaptosomes, it was found to be phosphorylated by a depolarization-induced calcium influx (Wu et al., 1982). The

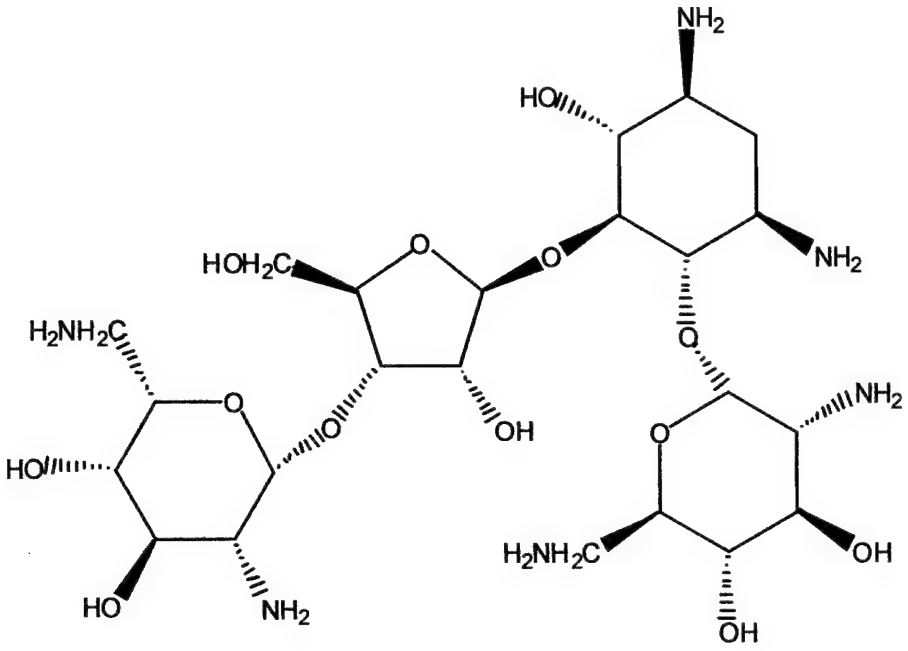

Figure 1.1-3: Chemical structure of Neomycin

phosphorylation reaction was found to be stimulated by calcium/phosphatidylserine and inhibited by calmodulin (Wu et al., 1982; Zolessi et al., 1999; Albert et al., 1986; Arbuzova et al., 1997). This stimulation by the calcium/phosphatidylserine was later attributed to the phosphorylation of the protein by Ca+/phospholipid/diacylglycerol-dependent protein kinase (protein kinase C) (Albert et al., 1986).

Initial studies of MARCKS in synaptosomes showed the protein acting as both a membrane associated protein as well as a soluble protein (Albert et al., 1986). The myristoylation on the N-terminus of the protein helps to anchor the protein to the membrane, but is not solely responsible for keeping the protein attached to the membrane (Aderem et al., 1988; James and Olson, 1989). For the protein to be membrane associated the myristolylation as well as the insertion into the membrane of five particular phenylalanine residues are necessary. Activation of protein kinase C and the resulting phosphorylation of MARCKS causes the protein's translocation from the membrane to the cytosol (Albert et al., 1986; Wang et al., 1989; James and Olson, 1989). The neutralization of the net charge on the protein, through this phosphorylation, and the resulting release from the membrane has been termed an "electrostatic switch". It is also known that the binding of MARCKS to calmodulin causes MARCKS to be released from the membrane surface (Albert et al., 1986; Wang et al., 1989; James and Olson, 1989; Arbuzova et al., 1997; Ohmitsu et al., 1999; Zolessi et al., 1999).

The portion of the MARCKS protein which contains the five phenylalanines, the four phosphorylation sites and the calmodulin binding site is called the phosphorylation site domain (PSD) or the effector domain (Blackshear, 1993; Zolessi et al., 1999; Qin and Cafiso, 1996; Yamauchi et al., 1998). This portion of the protein is highly conserved

between species including: human, cow, chicken, mouse and rat. The peptide derivative to be described here is from the sequence of the human MARCKS protein, contains amino acids 151-175, and has the following sequence:

KKKKKRFSFKKSFKLSGFSFKKNKK.

Electron paramagnetic resonance spectroscopy (EPR) and circular dichroism spectroscopy (CD) data have shown that the effector domain peptide MARCKS (151-175) exists as a random coil in solution (Qin and Cafiso, 1996; Arbuzova et al., 1997). The current proposed structure of the effector domain when bound to lipid membranes is shown in Figure 1.2-1. The peptide is in a primarily extended structure with the five phenylalanine residues turned into the lipid membrane and the N-terminus extending into the aqueous phase (Victor et al., 1999).

1.2.2 MARCKS interactions with other molecules

In addition to being a PKC substrate and a strong calmodulin binder, MARCKS binds to actin (Corradin et al., 1999; Yamauchi et al., 1998). MARCKS also inhibits the phospholipase C hydrolysis of the PIP_2 (Figure 1.2-2) (Wang et al., 2001; Arbuzova et al., 1997). Phosphorylation of the MARCKS peptide by PKC not only releases the peptide from the membrane but also reduces the peptide's affinity for calmodulin. The peptide may then reside in an equilibrium of three states; bound to the membrane, bound to calmodulin or in solution after phosphorylation by PKC. Therefore, it has been hypothesized that MARCKS controls the amount of free calmodulin by acting as a PKC regulated calmodulin buffer (Zolessi et al., 1999, Qin and Cafiso, 1996). More recently, MARCKS has been proposed to act to sequester PIP_2.

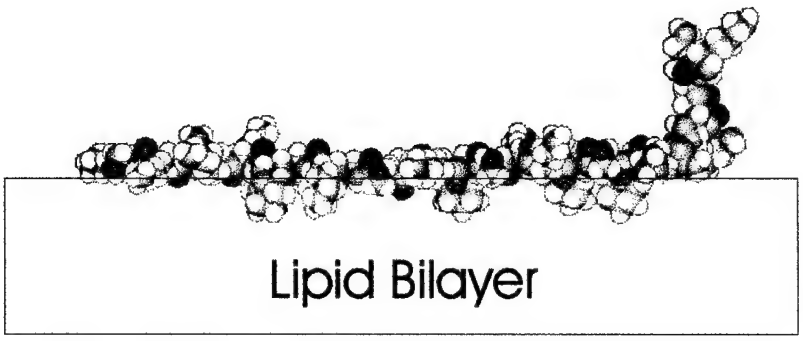

Figure 1.2-1: Proposed structure of MARCKS effector domain peptide when bound to lipid membrane (adapted from Victor, 1999)

1.2.3 Interactions with PIP_2

It is believed the MARCKS protein and MARCKS (151-175) peptide block the hydrolysis of PLC by binding to the PIP_2 lipid. This binding may be primarily electrostatic, because the MARCKS (151-175) peptide has a net charge of +13 whereas a molecule of PIP_2 has a net charge of –3 on the membrane at neutral pH. It has been hypothesized from results of both electrophoretic mobility measurements as well as competitive fluorescence binding experiments that MARCKS (151-175) forms approximately a 1:4 electroneutral complex with the PIP_2 lipid (Wang et al., 2001).

The experiments described in the following sections were undertaken to further characterize the interaction between the MARCKS effector domain and the acidic lipid PIP_2. If, as hypothesized, the binding of MARCKS to PIP_2 acts as a method to sequester PIP_2 until needed, then characterizing the MARCKS/ PIP_2 interaction is imperative for understanding how this regulatory mechanism functions.

1.3 Two additional acidic lipid binding molecules

1.3.1 Secretory carrier membrane protein (SCAMP)

In 1991 an antibody raised against parotid secretion granule membranes identified three cytoplasmic integral membrane proteins. These proteins, which are found in a diverse number of granule and vesicle membranes involved in secretion, were named secretory carrier membrane proteins (SCAMP) (Brand et al., 1991). SCAMPs are highly conserved across species and are found in all examined tissue and cell types (Wu and

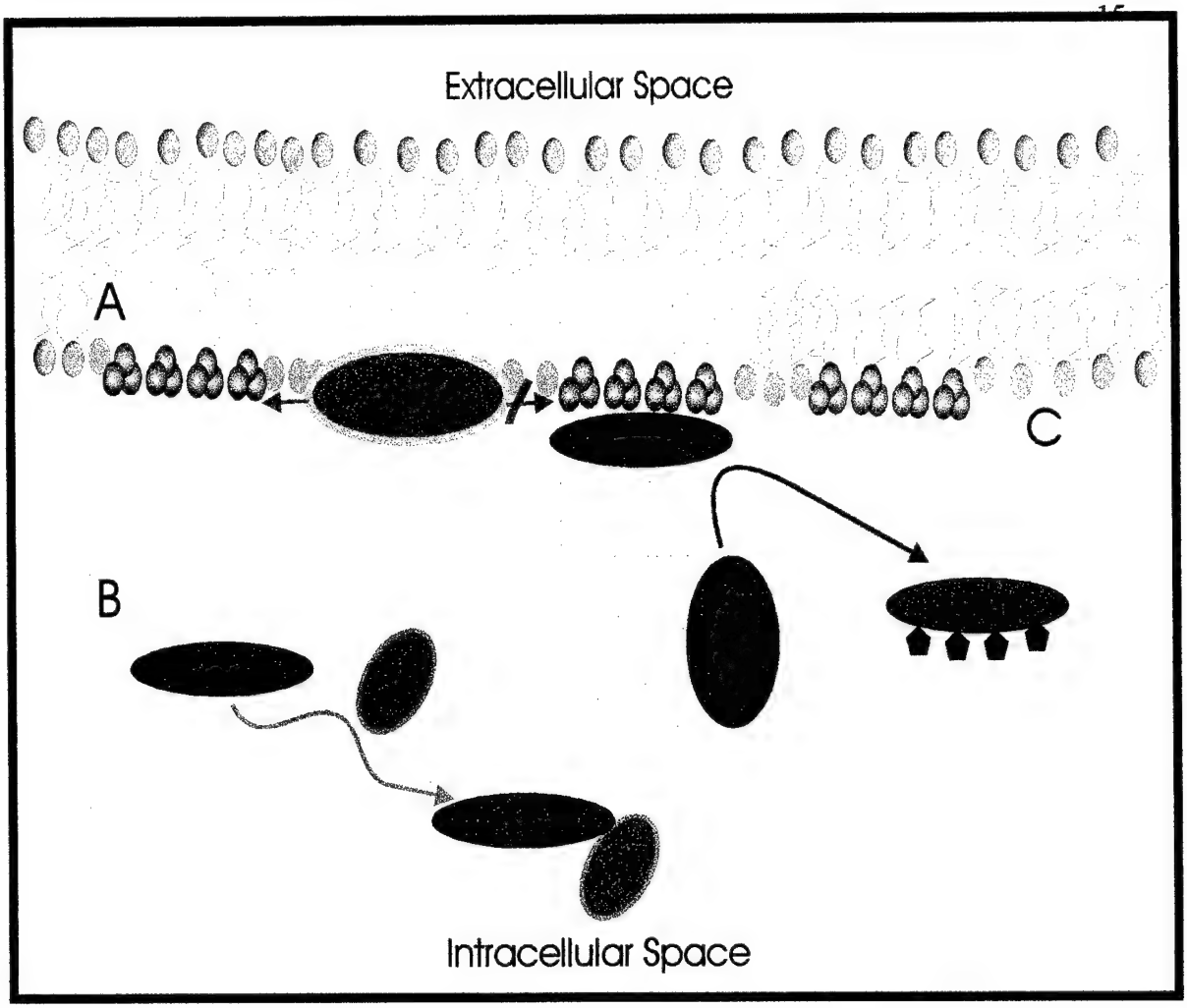

Figure 1.2-2: Known interactions of MARCKS protein within the cell. A) MARCKS blocks the PLC hydrolysis of PIP_2 B) MARCKS binds to Ca+Calmodulin C) MARCKS is released from the membrane surface through phosphorylation by PKC

Castle, 1997). Specifically, SCAMPs have been found in most membranes that recycle between cell surface and internal compartments including early and late endosomes, Golgi-derived vesicles, membranes that circulate various transporters and secretory granules and vesicles in hematopoietic cells (Hubbard et al., 2000). Although the exact role of SCAMPs within cells has still not been elucidated, the proteins do act as general markers of cell surface recycling pathways (Brand and Castle, 1993). In addition, there is evidence that SCAMPs may play a role in membrane trafficking leading to membrane fusion. Genetic knock-outs of SCAMP1 cause complications with exocytosis and upon addition of SCAMP peptide derivatives exocytosis is inhibited (Guo et al., 1999). SCAMP is an integral membrane protein with four membrane spanning domains. Both the N- and C- terminal portions of the protein are cytoplasmically oriented. There are three conserved amphiphilic segments which connect the transmembrane domains. Circular dichroism measurements indicate that the middle segment is between 20-30% α-helical whereas data for the first and last segments is indicative of β-sheet (Figure1.3-1) (Hubbard et al., 2000). A peptide corresponding to the segment linking transmembrane domains two and three has shown to be a strong inhibitor of exocytosis in permeabilized mast cells (data unpublished). This inhibition occurs late in the fusion process and is reversed by a four-fold molar excess of PIP_2. In addition to the reversal by PIP_2, the polyphosphoinositides PI4P and $PI3,4,5P_3$ were found to neutralize the effect of this peptide (data unpublished). EPR measurements indicate that the SCAMP peptide does binds to membranes containing PIP_2 however, the peptide has a much lower binding affinity to the phospholipid than MARCKS (151-175). The addition of 10nM of the MARCKS peptide completely inhibited PLC-δ1 hydrolysis of PIP_2 whereas 10μM of the

SCAMP peptide was required for complete inhibition (unpublished data). With the recent implications that PIP_2 is involved in exocytosis, a working hypothesis for the regulation of the lipid during membrane fusion involves the sequestering of PIP_2 by the SCAMP protein. Although this mechanism has yet to be fully understood, it is consistent with the developing theory that PIP_2 is regulated by proteins.

1.3.2 Pentalysine

Pentalysine is a peptide consisting of five consecutive lysine amino acids. Each lysine contains a positive charge on its amine group (Figure 1.3-2). Pentalysine does not bind to neutral lipid. There is experimental evidence that supports pentalysine binding to and forming lateral domains of PS and PIP_2 within membranes (Ben-Tal et al., 1996; Glaser et al., 1996). Bucki et al (2000) showed that in large unilamellar vesicles (LUVs) these acidic lipid domains formed at concentrations of up to 2mM of pentalysine. However, above that peptide concentration, the domains disassociated. The domain formation of the acidic lipid by pentalysine in LUVs has been disputed as an artifact of the experimental technique. Experiments using monolayers instead of LUVs did not show domain formation. Murray et al have suggested that the data supporting the presence of the domains is actually an artifact of vesicle aggregation. This aggregation is caused by the collapse of a vesicle onto another vesicle which has been charge neutralized by the binding of the peptide to the acidic lipid (Murray et al., 1999). While the ability of pentalysine to promote acidic lipid domains is disputed, data does show that pentalysine binds to acidic lipid. The positively charged pentalysine binds outside the polar headgroup of the lipid and with an apparent association constant of about $5.4 \times 10^3\ M^{-1}$ to

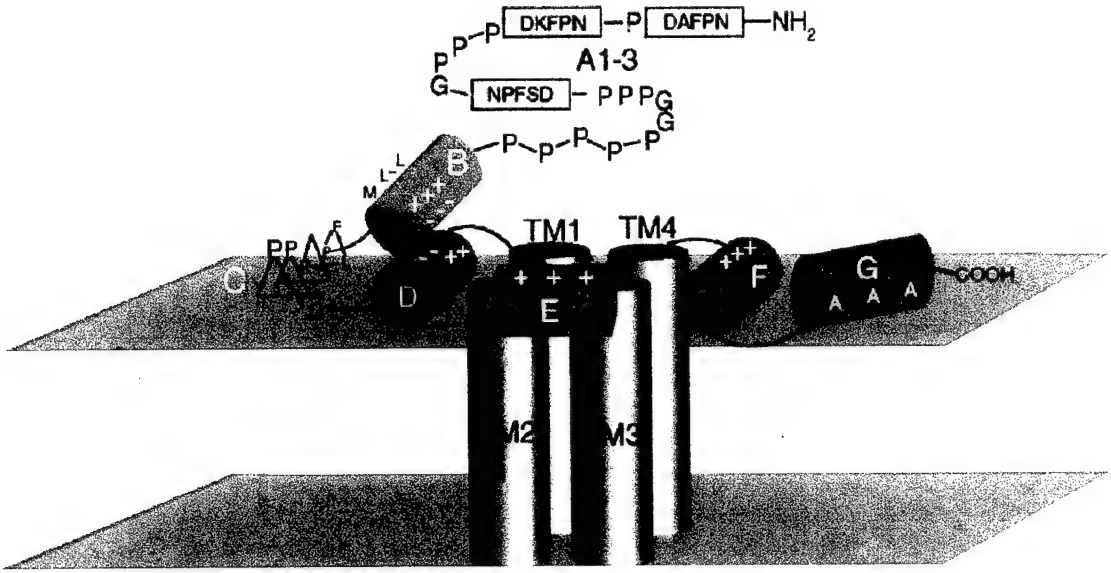

Figure 1.3-1: Proposed topology of SCAMP1 protein incorporating the four transmembrane segments and cytoplasmically oriented C-terminal and N-terminal portions (Hubbard et al., 2000).

lipid vesicles containing 33% acidic lipid (Ben-Tal et al., 1996). In addition to binding to PIP_2, there is some data that may suggest pentalysine blocks the hydrolysis of PIP_2 by PLC (Glaser et al., 1996).

1.4 Proposed Research

The diverse number of important cellular signaling systems that PIP_2 is involved in makes this lipid one of prime interest. There are several techniques that are often used to study binding interactions of lipids and their counterparts. However, each of them has restrictions that must be taken into account.

Nuclear magnetic resonance (NMR) spectroscopy is a powerful tool that can be used to unravel intricate interactions; however, a significant amount of sample is needed. Commercially, PIP_2 costs about $100-300 per milligram, making NMR an extremely expensive technique to use for this application. On the contrary, fluorescence spectroscopy requires only nanomolar concentrations of sample, and a fluorescently labeled PIP_2 (NBD-PIP_2) is commercially available. However, to ensure the lipid vesicles do not cause light scattering, the lipid concentrations must be kept very low. It has been found that at these nM concentrations the NBD-PIP_2 is not completely associated with the lipid vesicles. Without full incorporation of the NBD-PIP2 into the vesicles it is impossible to accurately measure the lipid's binding properties (Glaser et al., 1996). Electrophoretic mobility experiments suggest that multiple PIP_2 bind to a MARCKS peptide of the effector domain. However, in electrophoretic mobility experiments there is no way of determining the possible counterion binding which may influence the apparent stoicheometry (Wang et al., 2001). The other technique utilized

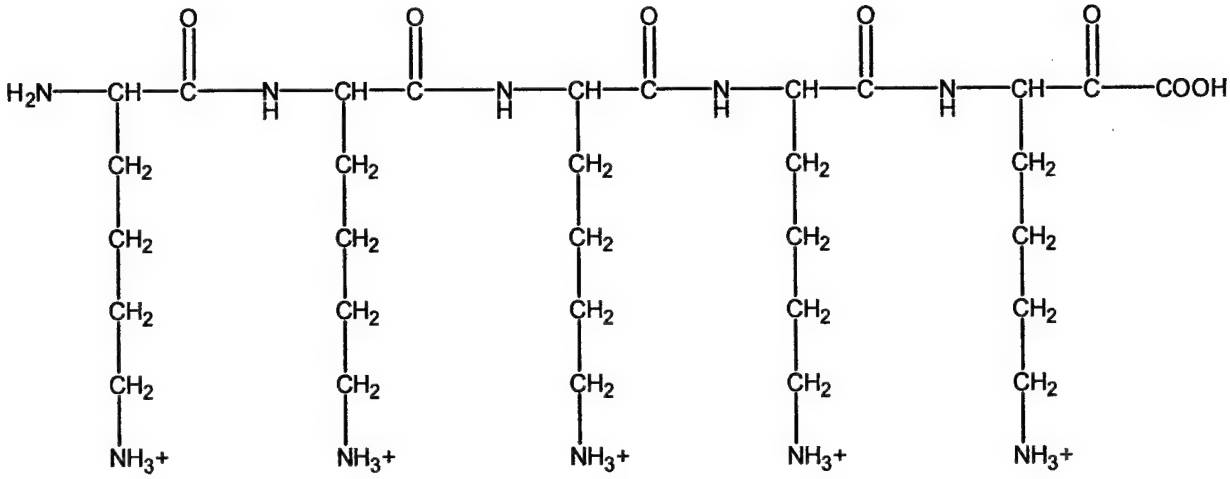

Figure 1.3-2: Structure of Pentalysine peptide

that indicates multiple PIP_2s bind to each MARCKS peptide is sucrose-loaded vesicle centrifugation (Wang et al., 2001). While this technique can certainly indicate binding activity, it gives no insight into specific binding mechanisms.

However, electron paramagnetic resonance spectroscopy (EPR) has fewer limitations; only micromolar concentrations of sample are needed, EPR is not affected by light scattering and the technique can be used to gain quantitative information on conformation, dynamics and associations. Therefore, EPR spectroscopy is an ideal choice for examining PIP_2 and its binding interactions within biologically relevant lipid vesicles.

The purpose of the research presented here is two-fold. The first goal is to characterize a spin-labeled PIP_2 molecule and document that it can be used in conjunction with EPR to probe PIP_2 interactions within lipid vesicles.

The second goal is to investigate the specific interaction between PIP_2 and the MARCKS effector domain peptide through EPR spectroscopy. This is achieved by first examining the binding of the proxyl-PIP_2 to the MARCKS (151-175) peptide and any resulting conformational or location changes in the proxyl-PIP_2. Characterization of the MARCKS-PIP_2 interaction is accomplished by analyzing the conformation and structure of several spin-label derivatized cysteine substituted MARCKS peptides in the presence and absence of PIP_2.

Chapter 2 Introduction into Electron Paramagnetic Resonance (EPR) Theory

2.1 Basic EPR Theory

Electron paramagnetic resonance (EPR) is a spectroscopic technique discovered in 1945 by Zaviosky that involves investigating the transitions introduced into the Zeeman levels of a paramagnetic system in a magnetic field (Nordio, 1976; Gordon and Breach, 1969). The basic theory describing this phenomena is discussed below.

An atom with an unpaired electron, also known as a paramagnetic species, will have a non-zero electronic angular momentum, **J** (Nordio, 1976; Gordon and Breach, 1969). The non-zero **J** gives rise to a magnetic dipole moment which is the combination of contributions from the spin angular momentum **S** as well as the original angular momentum **L** (Nordio, 1976). This magnetic electron moment, μ, is expressed by the equation:

$$\mu=-g\beta_e\mathbf{J} \tag{2-1}$$

where β_e is the Bohr magneton equal to $9.2733*10^{-21}$ erg/gauss, and g is the spectroscopic splitting factor equal to 2.00232 for a free electron (Robinson et al., 1985). For the nitroxide labels dealt with in our experiments, the magnetic contributions to **J** are primarily due to **S** allowing **L**=0. Therefore, the magnetic moment equation can be rewritten to account only for **S** contributions as:

$$\boldsymbol{\mu}=-g\beta_e\mathbf{S} \tag{2-2}$$

The interaction energy of this magnetic moment placed within an external uniform field **H** with an intensity H_o is expressed by the Hamiltonian operator:

$$\mathcal{H}=-\boldsymbol{\mu}\cdot\mathbf{H}=g\beta_e\mathbf{H}\cdot\mathbf{S}=g\beta\cdot H_o\,\mathbf{S}_z \tag{2-3}$$

For the systems which contain only one unpaired electron, S=1/2. By allowing m_s to be equal to the values of the components of $\mathbf{S_z}$ along the magnetic field direction quantum mechanics then dictates that m_s can assume only values of +1/2 or –1/2. The equation describing the interaction energy, W, then becomes:

$$W_{ms}=g\beta_e H_o m_s \tag{2-4}$$

The energy levels of the system can then be either:

$$W_{+1/2}= 1/2g\beta_e H_o \quad \text{or } W_{-1/2}=-1/2g\beta_e H_o \tag{2-5}$$

It then follows that the difference in energy between the two m_s states is:

$$\Delta W=W_{+1/2}-W_{-1/2}=g\beta_e H_o \tag{2-6}$$

Where ΔW, the Zeeman interaction energy, is the difference in the energy between the two levels created by the magnetic field, and is represented in Figure 2.1-1. If the sample is placed in an electromagnetic field of frequency ν_o, the excitation from the lower to higher state will occur when:

$$h\nu_o=g\beta_e H_o \tag{2-7}$$

In EPR spectroscopy the frequency is held constant and the magnetic field is scanned therefore it is convenient to rewrite Equation 2-6 as:

$$H_o=h\nu_o/g\beta_e \tag{2–8}$$

Most EPR spectrometers operate at a microwave frequency of about 9.5 GHz, also known as the X-Band. At this frequency magnetic resonance occurs at a magnetic field strength (g=2) of about 3,400 Gauss (G). The absorption energy and corresponding relaxation are the parameters being measured during EPR spectroscopy. However, because EPR spectroscopy is a phase dependent technique the EPR signal is recorded as

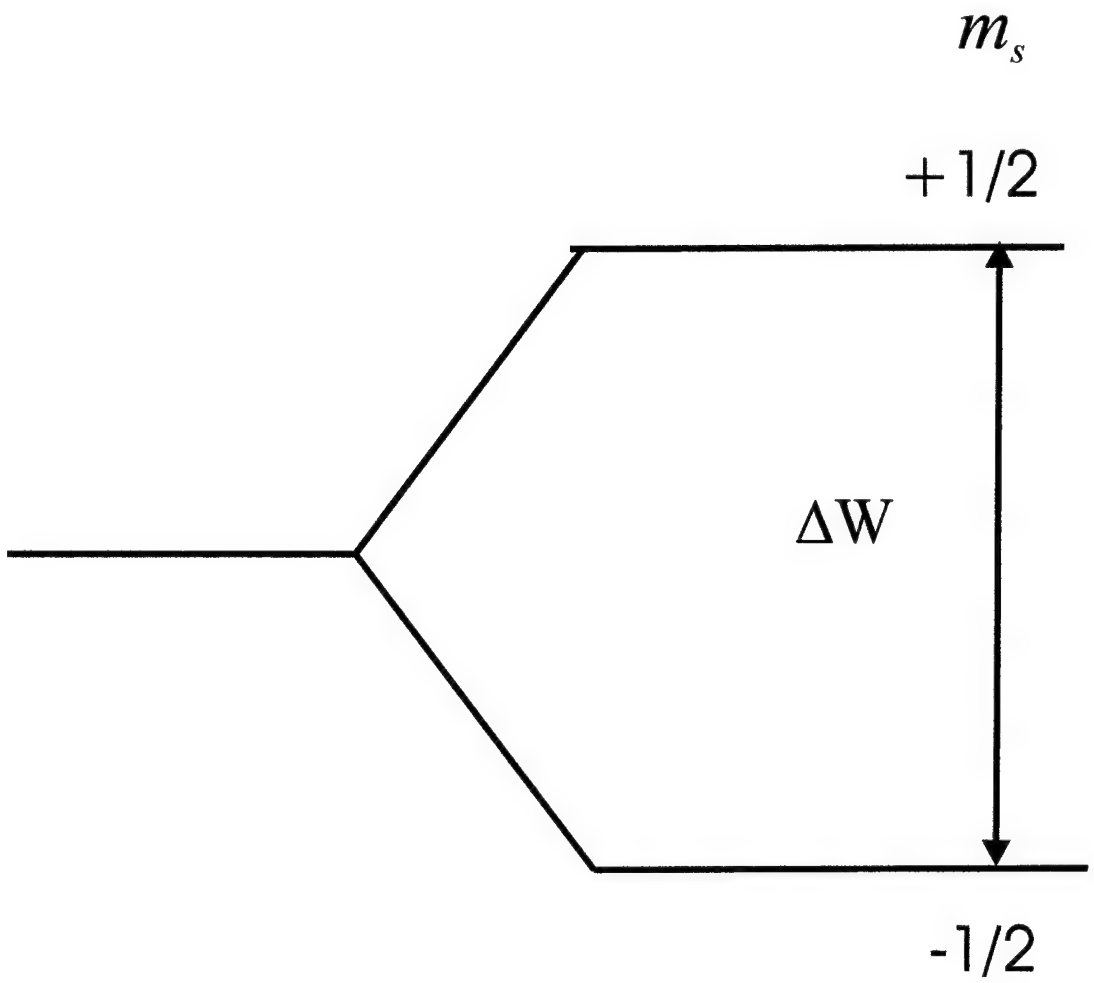

Figure 2.1-1 Zeeman splitting of an S=1/2 state

the first derivative of the absorption versus magnetic field. An example of the Lorentzian function absorption curve and corresponding first derivative are see in Figure 2.1-2.

2.1.1 Hyperfine Structure

Although EPR spectra are collected in the form of the first derivative of the absorption curve as seen in Figure 2.1-2, for nitroxide spin labels, spectra consist of multiple absorption peaks. These multiplet structures are the consequence of the interaction between the unpaired electron and the magnetic moments of the nuclei. This interaction is termed the hyperfine coupling and gives rise to the multiple spectral lines, or hyperfine structures. The number of energy levels and resulting hyperfine structures is determined by the specific atom type and the value of its non-vanishing nuclear spin angular momentum, I. $2I+1$ orientations are allowed for the nuclear spin and for nitrogen, $I=1$, therefore the three allowed orientations result in three hyperfine lines. As seen in Figure 2.1-3 the allowable transitions, following the selection rules $\Delta m_s = \pm 1$ and $\Delta m_I = 0$, are now $m_I = -1$, 0, and 1. These three possible transitions give rise to not one absorption line but three upon excitation of the unpaired electron.

2.1.2 Anisotropic Contributions

For most nitroxide radicals the Lande factor, g_e, introduced earlier has an approximate value of 2. This approximation assumes that the orbital angular momentum of the molecule is essentially zero ($\mathbf{L} \approx 0$). However, when the paramagnetic molecule is placed within a magnetic field the combination of the magnetic field and the spin-orbital coupling reintroduces small contributions of orbital angular momentum into the ground

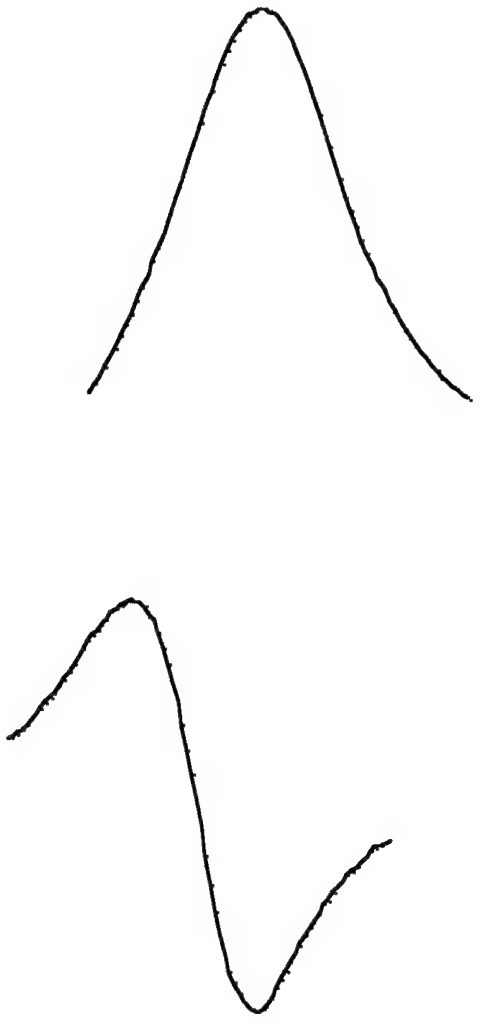

Figure 2.1-2 Lorentzian function absorption curve (top) and corresponding first derivative (bottom)

state. This induced orbital angular momentum causes deviations in the g_e factor from the free-spin value. Since, the magnitudes of the deviations from the g_e factor are dependent upon the orientation of the molecular axis with respect to the magnetic field, the g_e factor can no longer be scalar but must be represented by a 2nd rank tensor. The **g** tensor is a symmetric tensor whose elements are composed of the free-electron g_e value plus an anisotropic correction due to the spin-orbital coupling.

The hyperfine coupling tensor, the **A** tensor is also a symmetric 2nd rank tensor. When a molecule is placed within a magnetic field the nuclear spins quantize. The electron experiences the combined effect of the external magnetic field and the field at the electron due to the induced nuclear magnetic moments. The **A** tensor contains an isotropic contribution arising from the Fermi contact term (determined by the electron density at the nucleus) and an anisotropic contribution due to the dipole-dipole interaction between the unpaired electron and the nuclear magnetic moment. The values of the principle components of the **A** tensor are also dependent upon molecular orientation with respect to the magnetic field.

2.1.3 Site-directed spin-labeling

Not all molecules have stable unpaired electrons thus in order to exploit the characteristics of a free electron through EPR spectroscopy, it is necessary to introduce a stable free radical into the macromolecule of interest. One manner of doing this is site-directed spin-labeling. An extraordinarily useful EPR technique, site-directed spin-labeling (SDSL) can deduce quantitative and qualitative information about protein structure, motion and interactions{Garber, 1999 #1; Altenbach, 1989 #35; Altenbach,

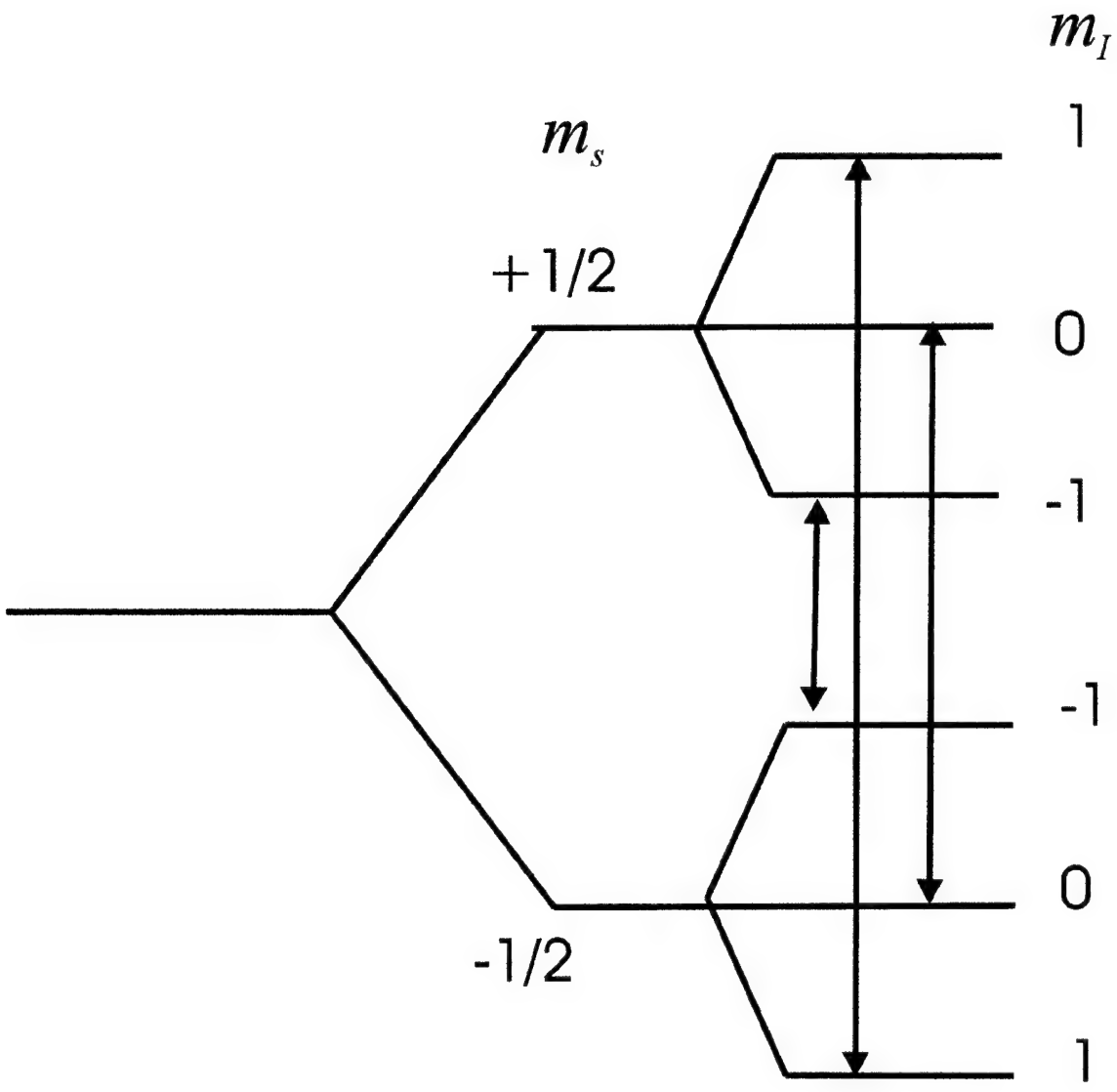

Figure 2.1-3 Energy levels with splitting caused by hyperfine coupling with nuclear spin of I=1. Arrows indicate allowed transitions.

1994 #34; Mchaourab, 1997 #10; Jiang, 1997 #11}. SDSL either utilizes a native cysteine within a protein or requires the replacement of one amino acid within a protein or peptide sequence with a cysteine. This cysteine is then reacted with a sulfur containing spin-label through a disulfide bond (Figure 2.1-4). Through analysis of the motion of the spin-label as well as its collisional frequency with various paramagnetic agents, EPR spectroscopy of a spin-labeled protein can be used to determine secondary structure of a protein in solution or when bound to lipid membranes, possible tertiary structures, binding characteristics and affinities, as well as electrostatic potential at membrane surface sites (Hubbell and Altenbach, 1994; Klug et al., 1997; Altenbach et al., 1994; Altenbach et al., 1989; Kim et al., 1997).

2.2 EPR techniques

2.2.1 Analysis of spectrum lineshape

The EPR spectral lineshape indicates the motion of the spin-labeled side chain as well as that of entire spin-labeled molecule (Mchaourab et al., 1997). Any changes in tertiary interactions will result in a change in the dynamics of the spin label and hence effect the lineshape of the EPR spectrum (Mchaourab et al., 1996). Therefore, careful analysis of the EPR spectrum can give insight into changes in the environment of the spin-labeled molecule. Rotational correlation time, τ_c, is a measure of the length of time over which molecules exist in a given orientation (Poole and Farach., 1987). Changes in rotational correlation time indicates changes in the average orientation and configuration of the molecule with respect to the magnetic field. These changes may result from solvent interactions with or conformational changes of the molecule. The rotational

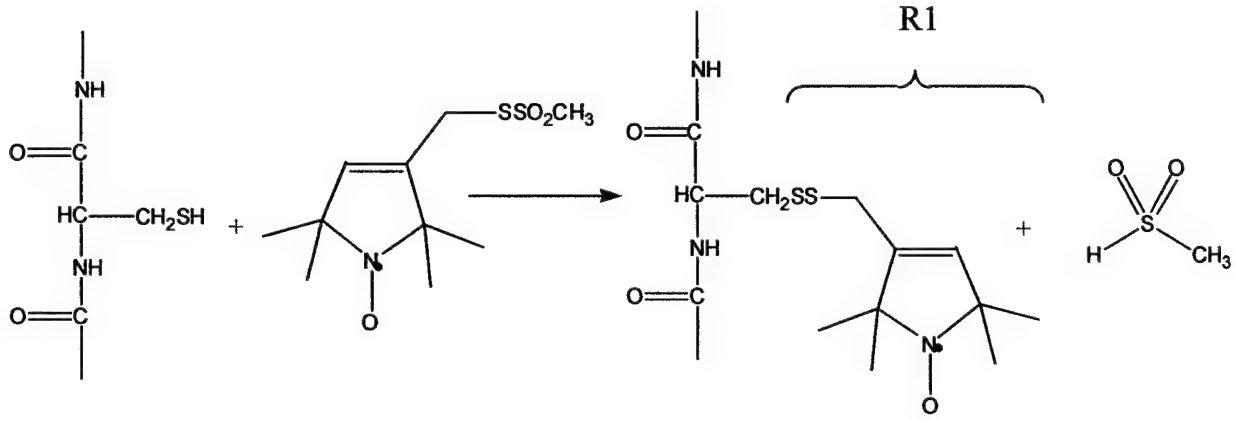

Figure 2.1-4 Site directed spin labeling with methanethiosulfonate spin label (MTSSL)

correlation time is related to the mean time of the existence of any particular molecular configuration. The rotational correlation time of a molecule containing a nitroxide spin-label can be estimated by analysis of the molecule's EPR spectrum using equation (2-9).

$$\tau_c \approx \frac{\sqrt{3}}{2} * \Delta H_{m=0} * \sqrt{\frac{A_{m=0}}{A_{m=-1}}} \qquad (2\text{-}9)$$

Where $\Delta H_{m=0}$ is the peak to peak line with of the central peak and $A_{m=0}$, $A_{m=-1}$ are the peak to peak amplitude values for the central and high field peaks respectively. An increase in correlation time caused by the slower tumbling of the molecule, will result in a broadening of the EPR spectrum. Possible causes for an increased correlation time can be changes in the rotation or flexibility of the spin label.

In addition to information about the motion of the molecule as a whole, an EPR spectrum can give information about the location of the spin-labeled molecule with respect to other spin-labeled molecules. Dipolar broadening caused by spin-spin interactions may lead to lineshape broadening. Exchange interactions between spins will narrow the lineshape at the center of the peak, causing it to be more Lorentzian, while the wings of the curve become broadened and more Gaussian. Simple analysis of the changes in spectrum lineshape can give insight into the forces acting on the molecule. Lineshape analysis, along with any of the techniques discussed below becomes a powerful analytical tool.

2.2.2 Power saturation

The location of a specific protein residue with respect to the membrane bilayer as well as secondary structure of a membrane protein can be determined using site-directed

spin-labeling in conjunction with an EPR technique called power saturation. If the microwave power in an EPR experiment is increased the number of electron spins in a higher energy level will approach the number at the lower energy level. The population excess in the ground state will ultimately be eliminated and no further net absorption can occur. At this point the system is said to be "saturated". The point at which saturation is reached is dependent upon a competition between power absorption and spin relaxation. Spin relaxation occurs as a result of interactions between the electron spins and their environment, which promotes a loss of energy from the excited state (Gordan and Breach, 1969}. There are two relaxation pathways in which the spin in the excited state can relax back to the ground state by the exchange of energy. The first, known as spin-lattice relaxation or T_1, is the transfer of energy from the paramagnetic species to the surrounding environment. The second is the spin-spin or dipolar broadening interaction, where the total energy of the spin system is maintained and the exchange is between like paramagnetic species. This spin-spin interaction is known as the T_2 relaxation.
For a single homogenous Lorentzian line the peak to peak amplitude of the first derivative adsorption spectrum, Y', has the form:

$$Y' \propto \frac{H_1}{\left(1 + H_1^2 \gamma^2 T_1 T_2\right)^{1.5}} \tag{2-10}$$

Where H_1 is the microwave magnetic field component in gauss, γ is the gyromagnetic ratio of the electron, and T_1 and T_2 are the spin-lattice and spin-spin relaxation times, respectively. In a microwave resonator, H_1 is proportional to the square root of the incident microwave power, P.

$$H_1 = \Lambda P^{1/2} \tag{2-11}$$

Where Λ is a constant depending on the properties of the resonator. Substituting $P^{1/2}$ into equation 2-8 for H_1 it can be seen that at very low power the signal increases as $P^{1/2}$, whereas at a high power it decreases as $1/P$. When the system begins to saturate the amplitude begins to deviate from the square root dependency on power. The amplitude will reach a maximum value and start to decrease.

A parameter used to describe the saturation behavior of a sample is $P_{1/2}$. $P_{1/2}$ is the microwave power require to saturate the signal to half the amplitude it would have if it did not saturate.

$$P_{1/2} = \frac{2^{2/3} - 1}{\Lambda^2 \gamma^2 T_1 T_2} \tag{2-12}$$

Therefore, determination of $P_{1/2}$ allows for estimation of the spin-lattice relaxation and spin-spin relaxation product.

Collision of the magnetic species with a fast-relaxing paramagnetic species results in a spin exchange and an increase of the nitroxide relaxation rate $1/T_1$ in proportion to the collision frequency such that:

$$\frac{1}{T_1} - \frac{1}{T_1^o} = fp\omega_e \tag{2-13}$$

where ω_e is the collision frequency, f, is a statistical factor, p is the collision efficiency, and $1/T_1^o$ is the relaxation rate in the absence of a relaxation agent. It can therefore be concluded that the change in $P_{1/2}$ due to the presence of a relaxation agent is proportional to the collision frequency.

$$\Delta P_{1/2} = P_{1/2} - P_{1/2}{}^o \propto \frac{1}{T_1 T_2} - \frac{1}{T_1^o T_2^o} \propto \frac{\omega_e}{T_2^o} \tag{2-14}$$

The rate of spin-spin relaxation is usually much faster than the collision rate, therefore T_2 is considered a constant. This allows $\Delta P_{1/2}$ to reflect relative collision frequency and therefore accessibility.

If the spin-label is exposed to and collides with a paramagnetic relaxation agent, the resulting spin-lattice interaction provides a mechanism for the spin to return to the ground state {Klug, 1997 #26}. To investigate the location of a spin-label within the membrane bilayer, one can choose paramagnetic relaxation agents which partition differently. This difference in location will give rise to different collision frequencies with the spin-labeled molecule. The ratio of the $\Delta P_{1/2}$ values of two agents, can be used to estimate Φ, a value that provides a depth such that :

$$\Phi = \ln\left(\frac{\Delta P_{1/2}(1)}{\Delta P_{1/2}(2)}\right) \tag{2-15}$$

When used in conjunction with a calibration curve of known depths and corresponding Φ values, the location of the spin-labeled species within the bilayer can be measured. Two commonly used paramagnetic relaxation agents are oxygen and nickel (II) ethylenediaminediacetic acid (NiEDDA). Oxygen, being non-polar, more readily penetrates the lipid bilayer. NiEDDA, being not only polar but also larger, cannot penetrate the lipid bilayer as deeply as oxygen. The partitioning characteristics of these two species makes them wise choices for use with power saturation involving lipid membranes.

To analyze the power saturation data that will be described here, the peak to peak height of the central line was plotted versus the square root of the power. These curves were then fit with the function:

$$A = IP^{1/2}\left[1+\frac{\left(2^{1/\varepsilon}-1\right)P}{P_{1/2}}\right]^{-\varepsilon} \qquad (2\text{-}16)$$

where A is the amplitude of the peak to peak height of the central line, I is a scaling factor, ε is a homogeneity factor and $P_{1/2}$ is the half-saturation value. Φ values were then calculated using Equation 2-13 above.

2.2.3 Titration

The binding specificity of a spin-labeled molecule to another molecule can be determined using EPR spectroscopy by analyzing the titration of one species into the other. By following the changes in amplitude and linewidth from the unbound spin labeled species to the fully bound species, it may be possible to deduce the binding affinity as well as stiocheometry (Wang et al., 2001).

If the two molecule of interest are at equilibrium between the free and bound states this can be described as:

$$A + B \leftrightarrow A\bullet B \qquad (2\text{-}17)$$

Where A and B are the unbound molecules and A•B is the 1:1 complex. Then the apparent association constant, K_a for 1:1 binding of A and B is written as:

$$K_a = [A\bullet B]/([A][B]) \qquad (2\text{-}18)$$

If $[A]_T$ is the total concentration of A in the system and $[B]_T$ is the total concentration of B in the system then it follows that:

$$[A]_T = [A]+[A\bullet B] \qquad (2\text{-}19)$$

$$[B]_T = [B]+[A\bullet B] \qquad (2\text{-}20)$$

and therefore it follows that:

$$[A] = [A]_T - [A \bullet B] \tag{2-21}$$

$$[B] = [B]_T - [A \bullet B] \tag{2-22}$$

Substituting equations 2-19 and 2-20 into equation 2-16 gives rise to equation 2-23:

$$K_a = \frac{[A \bullet B]}{([A]_T - [A \bullet B])([B]_T - [A \bullet B])} \tag{2-23}$$

Equation 2-23 is simplified to the following quadratic equation that will predict the 1:1 binding curve of the two complexed species:

$$[A \bullet B]^2 + [A \bullet B](-[A]_T - [B]_T - K_a^{-1}) + [A]_T[B]_T = 0 \tag{2-24}$$

Using the solution of equation 2-24 and equation 2-22 an expression to predict the amplitude of the central EPR resonance amplitude, $A_{m=0}$ as a function of added binding species can be adapted:

$$A_{m=0} = \frac{[B]}{[B]_T} A_f + \frac{[A \bullet B]}{[B]_T} A_b \tag{2-25}$$

Where A_f and A_b represent the intrinsic amplitudes of free and bound species associated with its spin-labeled counterpart. Likewise, for molecules that bind in a ratio greater than 1:1, as is the hypothesis for the PIP_2-MARCKS interaction, the following equilibrium equation is substituted:

$$A + (B)_n \leftrightarrow A \bullet (B)_n \tag{2-26}$$

This equilibrium equation assumes A and multiple B bind in a single step. A quadratic is derived which compensates for the binding of more than one molecule "B" by incorporating the assumption of Equation 2-26 instead of Equation 2-17 which can then be used to predict the amplitude of the central EPR resonance amplitude, $A_{m=0}$ as a function of added binding species when A binds to multiple B.

2.2.4 Low temperature EPR

Additional information regarding dipole interactions between spin labels can be obtained by freezing the sample. This technique can give information on the distance or changes in distance between pairs of nitroxide spin labels (Mchaourab et al., 1997). By freezing the sample it is possible to eliminate the motion of the spin label and therefore the motion's contribution to the EPR spectral lineshapes (He et al., 1997; Rabenstein and Shin, 1995). In addition, if the lineshape of an EPR spectrum is determined by spin-lattice interactions, as the temperature drops and motion of the molecule slows, the total contribution of these interactions to the lineshape will decrease. However, if spin-spin interactions play a dominant role in determining the spectrum lineshape, the temperature dependence of the spectrum lineshape will be minimal (Al'Tshuler and Kozyrev, 1964). At the lower temperature, -40C for the samples to be described here, it is possible to differentiate between samples that have spin labels close enough in proximity to have dipole interactions and those that do not (Wang et al., 1998; Gross et al., 1999). By calculating the line height ratio d_1/d (Figure 2.2-1) of the EPR spectrum of a frozen sample, it is possible to obtain an approximate estimate of the interspin distance. The distance determined can be the distance between two separately labeled molecules, or the distance between two spins located on the same molecule. A value of <0.4 for d_1/d is expected when no spin-spin interaction exists. A value of 0.4 and greater indicates spin-spin proximity starting at 24 Å and decreasing in distance (Wang et al., 1998).

Chapter 3 Materials and Methods

3.1 Materials

3.1.1 Phospholipids

Spin labeled phosphotidylinositol (4,5) bisphosphate triethylammonium (proxyl-PIP_2) a novel probe for studying the properties of membrane bound PIP_2 was synthesized at our request by Colin Ferguson in the laboratory of Glenn Prestwich (University of Utah)(Figure 3.1-1). The proxyl-PIP_2 was dissolved in chloroform for experimental use. L-α-phosphatidylcholine (egg) and phosphatidylserine (brain sodium salt) were purchased as chloroform solutions from Avanti Polar Lipid (Alabaster, AL) and were used without further purification. L-α-phosphatidyl-D-myo-inositol-4,5-bisphosphate was purchased as a powder from Boehringer Mannheim (Germany) and was dissolved in 4:4:1 chloroform, methanol, water before use.

3.1.2 Peptides

Pentalysine was purchased from Sigma Chemical Co (St. Louis, MO). A secretory carrier membrane protein peptide comprised of amino acids 230-240 of the bovine SCAMP 2 protein with the sequence: non-acetylated-C-W-Y-R-P-I-Y-K-A-F-R-amide was synthesized by the University of Virginia Biomolecular Research Facility (Charlottesville, VA). The native myristolyated alanine rich c-kinase substrate (151-175) (MARCKS) peptide and six cysteine mutant peptides were also synthesized by the University of Virginia Biomolecular Research Facility. The native MARCKS (151-175) peptide had the following sequence: Ac-K-K-K-K-K-R-F-S-F-K-K-S-F-K-L-S-G-F-S-F-K-K-N-K-K- amide. The six mutants had the following substitutions: K3C, S12C,

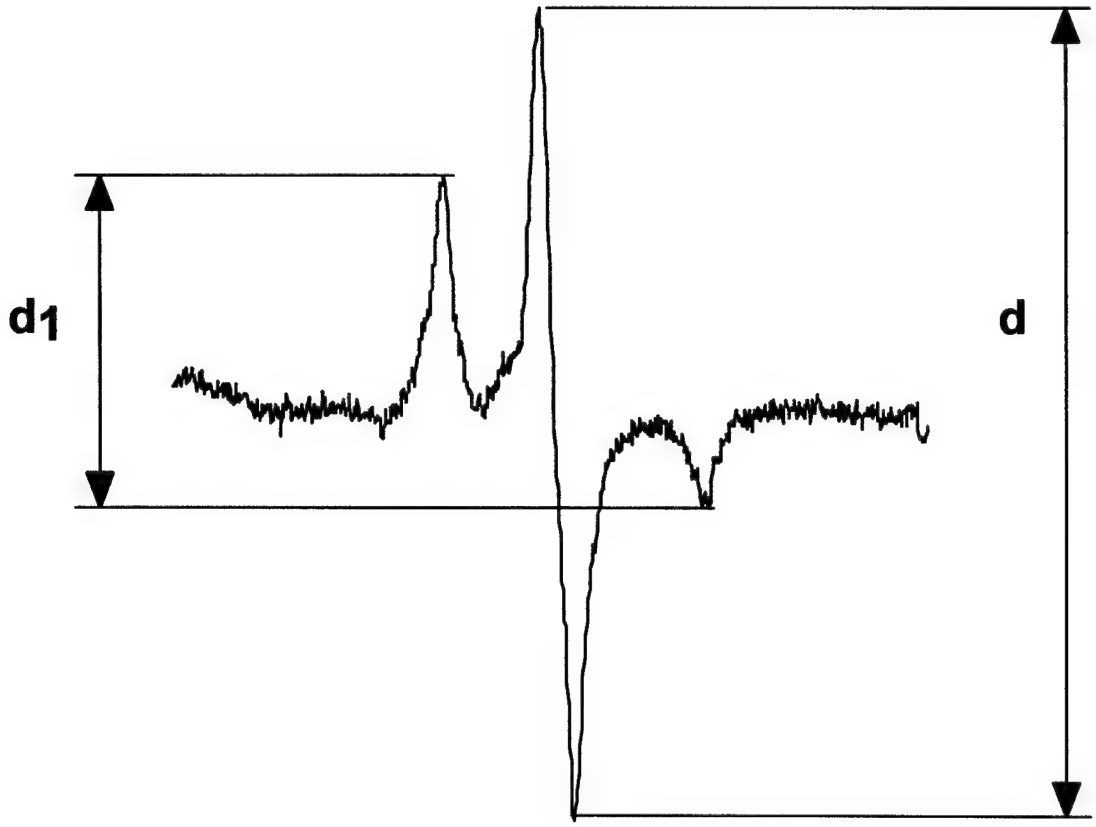

Figure 2.2-1 Low temperature EPR spectrum showing measurements d and d_1. If the ratio d_1/d is >0.4 it is an indication there is a dipolar interaction between two spins in close (within 24 Å) proximity

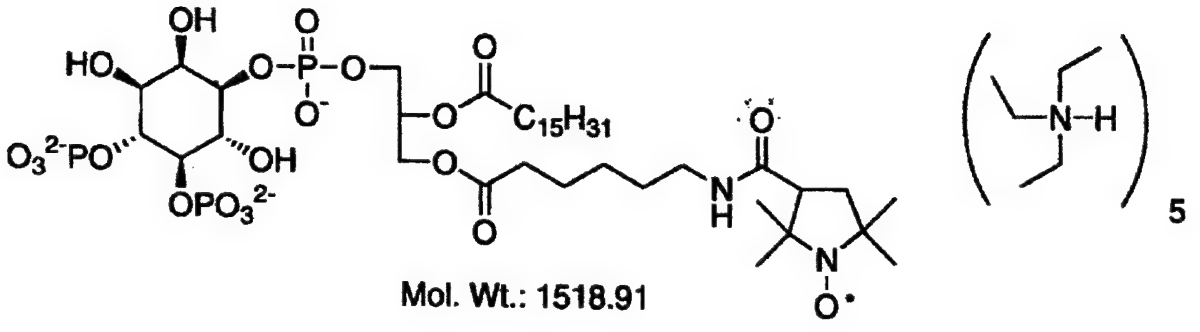

Figure 3.1-1 Chemical structure of proxyl-PIP_2

S16C, N23C, S8C/S12C and S16C/S19C. The native MARCKS (151-175) was used as purchased. The MARCKS cysteine derivatives peptides were spin-labeled with methanethiolsulfonate and purified using an AKTA Purifier from Amersham Pharmacia Biotech (Piscataway, NJ) fitted with a R2/10 POROS reverse phase column from PerSpective Biosystems (Framington, MA) using a 0-80% Acetonitrile / ddH_2O gradient, with the major peak eluting at approximately 60% Acetonitrile. Further purification of the spin-labeled peptides was performed using a 3,000 molecular weight cut off (MWCO) Centricon centrifugal filter device from Millipore (Bedford, MA). Peptide identity was confirmed through electrospray ionization mass spectrometry.

Three single and seven double additional MARCKS (151-175) cysteine derivative peptides with the following substitutions: S8C, F9C, S19C, S8C/S19C, S8C/F20C, K10C/G17C, K10C/K21C, K11C/F18C, S12C/S19C, K14C/K21C were synthesized, spin-labeled and purified by high performance liquid chromatography (HPLC) by Karen Zaiger as described by Qin & Cafiso (1996).

3.1.3 PLCδ_1 PH domain protein

The clone of the PH domain from Human PLC-δ_1 (pET19bPHPLC-δ_1) was a gift from Dr. Mario Rebecchi (SUNY, Stony Brook, NY). The PCR kit was purchased from Perkin- Elmer (Norwalk, CT). Restriction enzymes, Taq DNA polymerase and T4 DNA ligase were purchased from New England Biolabs (Beverly, MA). The Altered Sites II in vitro Mutagenesis System and the JM109 and ES 1301 bacterial strains were from Promega (Madison, WI). Plasmid isolation kits and purification kits were purchased from Bio-Rad (Hercules, CA), Qiagen (Valencia, CA). The Hi-Trap 5ml chelating

column was purchased from Amersham Pharmacia Biotech (Piscataway, NJ). The nickel sulfate (hexahydrate) for charging the chelating column was purchased from Sigma Chemical Company (St. Louis, MO). Oligonucleotides were synthesized at the Core Facility (University of Virginia, Charlottesville, VA) as well as Integrated DNA Technologies (Coralville, IA). *Pfu* DNA polymerase was purchased from Stratagene (La Jolla, CA). The expression plasmids pET- 19b and pET-16b were from Novagen (Madison, WI). The *Escherichia coli* strain BL21 (DE3) was purchased from Novagen. DNA sequencing was performed at the Core Facility (University of Virginia, Charlottesville, VA).

3.1.4 Other materials

Neomycin sulfate was purchased from Calbiobiochem (La Jolla, CA). [1-Oxy-2,2,5,5-Tetramethyl-D-Pyrroline-3-Methyl] Methanethiolsulfonate (MTSL) spin label was purchased from Toronto Research Chemicals Inc. (Ontario, Canada). The TPX tubes used for the power saturation experiments were purchased from Medical Advances Inc. (Milwaukee, WI). Supracil and quartz capillary tubes were purchased from VitroCom Inc. (Mt. Lakes, NJ) and were heat sealed at the bottom for all spectra except the titration experiments. Chloroform was purchased from J.T. Baker (Phillipsburg, NJ). 3-[N-Morpholino]propanesulfonic acid (MOPS) sodium salt was purchased from Sigma (St. Louis, MO). Nickel acetylacetonate hydrate (NiAcAc) was purchased from Aldrich (Milwaukee, WI). Sulfuric acid and potassium chloride were from Mallinckrodt (Paris, KY). Ammonium molybdate tetrahydrate and acorbic acid were purchased from Fluka

(Milwaukee, WI). Methanol, sodium monobasic phosphate and 30% hydrogen peroxide were all purchased from Fischer (Fair Lawn, NJ).

3.2 Methods

3.2.1 Lipid vesicle preparation

Large unilamellar vesicles were made by first drying off the chloroform from the appropriate lipid in a pre-weighed round bottom flask on a rotary evaporator. For vesicles containing more than one type of lipid, the flask was weighed after drying off the chloroform from the first lipid and the next lipid/chloroform solution was added, vortexed and dried on the rotary evaporator. The lipid was then hydrated with 100 mM KCl 10 mM MOPS pH 7.0 buffer. The lipid suspension was freeze/thawed five times in liquid nitrogen and then extruded through 1000 Å polycarbonate filters (Poretics, Livermore, CA) using a LiposoFast extruder (Avestine, Ottawa, Canada).

3.2.2 EPR data acquisition

All room temperature spectra were obtained at the X-Band using an E-line series Varian spectrometer fitted with a loop-gap resonator using an incident microwave power of 2 mW, modulation amplitude of 1.25 gauss and field sweep of 100 gauss. All low temperature EPR spectra were acquired on the Varian spectrometer using a microwave power of 2 mW, modulation amplitude of 1.25 gauss and field sweep of 200 gauss.

All samples used for power saturation experiments were placed in a gas permeable TPX tube for data collection. Power saturation data of all proxy-PIP_2 experiments were taken by recording the central first derivative resonance as the

microwave power was increased from 0.25-80mW at a modulation amplitude of 1.25 and field sweep of 100 gauss. Power saturation data of spin-labeled MARCKS (151-175) mutants: K3R1, S12R1 and S19R1 were taken in the same manner. For all samples, baseline data was taken while flushing with nitrogen to ensure the absence of any secondary paramagnetic species. For all samples, 20% oxygen was flushed through the samples as the non-polar paramagnetic relaxing agent and unless otherwise noted 20mM NiAcAc was used in as the polar paramagnetic relaxing agent.

3.2.3 PLCδ_1 PH domain protein expression and purification

The PLCδ_1 PH domain protein was expressed and purified as seen previously (Tall et al., 1997) with only a few modifications. The cell lysate containing the expressed protein was purified on a AKTA Purifier from Amersham Pharmacia Biotech using a Hi-Trap 5 ml chelating column charged with nickel sulfate. The purified protein was eluted at approximately 400mM imidazole using a gradient of 5-1000 mM imidazole in 0.5 M NaCl 20 mM Tris pH 2.9. The identity of the purified PLC δ1 PH domain protein was verified through SDS-PAGE gel electrophoresis and mass spectroscopy.

3.2.4 Quantitation of proxyl-PIP2 concentration

The proxyl-PIP_2 was dissolved in chloroform and a Fiske-Subbarow phosphate assay performed to insure correct concentration (Fiske and Subbarow, 1925). An inorganic phosphate standard curve was prepared using known volumes of 5.2 mM sodium phosphate buffer. The standard samples and 1 µl PIP_2-sl solution were placed in clean disposible test tubes. 200 µl of 10% (v/v) sulfuric acid was added to each. The test

tubes were placed in a 200° C heating block. After one hour 25 µl of 30% H_2O_2 was added directly into the tubes while still in the heating block. Tubes were heated for an additional 40 minutes. Tubes were removed from the heating blocks and cooled to room temperature. While tubes were cooling color reagent was prepared (0.5 ml 5% ammonium molybdate in H_2O (w/v), 4.5 ml H_2O, 0.1g Ascorbic acid per 10 tubes). Once at room temperature 480 µl H_2O was used to rinse down the side of each tube. Each tube was vortexed after the rinse. 500 µl of color reagent was then added directly to the sample and the sample vortexed. The tubes were then incubated in a 45°C water bath for 20 minutes. The absorbance of each sample was read at 820 nm on a Hewlett Packard diode array UV-Vis spectrometer. The standard samples were used to calculate a standard curve (Figure 3.2-1) which was then used to calculate the concentration of the proxyl-PIP_2/chloroform solution.

3.2.5 Proxyl-PIP_2 characterization

EPR spectra of the proxyl-PIP_2 were taken when dissolved in chloroform, in aqueous solution and when incorporated into both 20mM PC and PC:PS (9:1) vesicles both with and without MARCKS(151-175).

3.2.6 Proxyl-PIP_2 titrations

The proxyl-PIP_2 was incorporated into the outside of the vesicles by first drying the lipid in a round bottom flask and removing the chloroform on a the rotary evaporator. The phosphatidylcholine (PC) vesicles were then added to the dry PIP_2. The solution was vortexed to incorporate the spin-labeled lipid into the vesicles. A surprasil capillary was

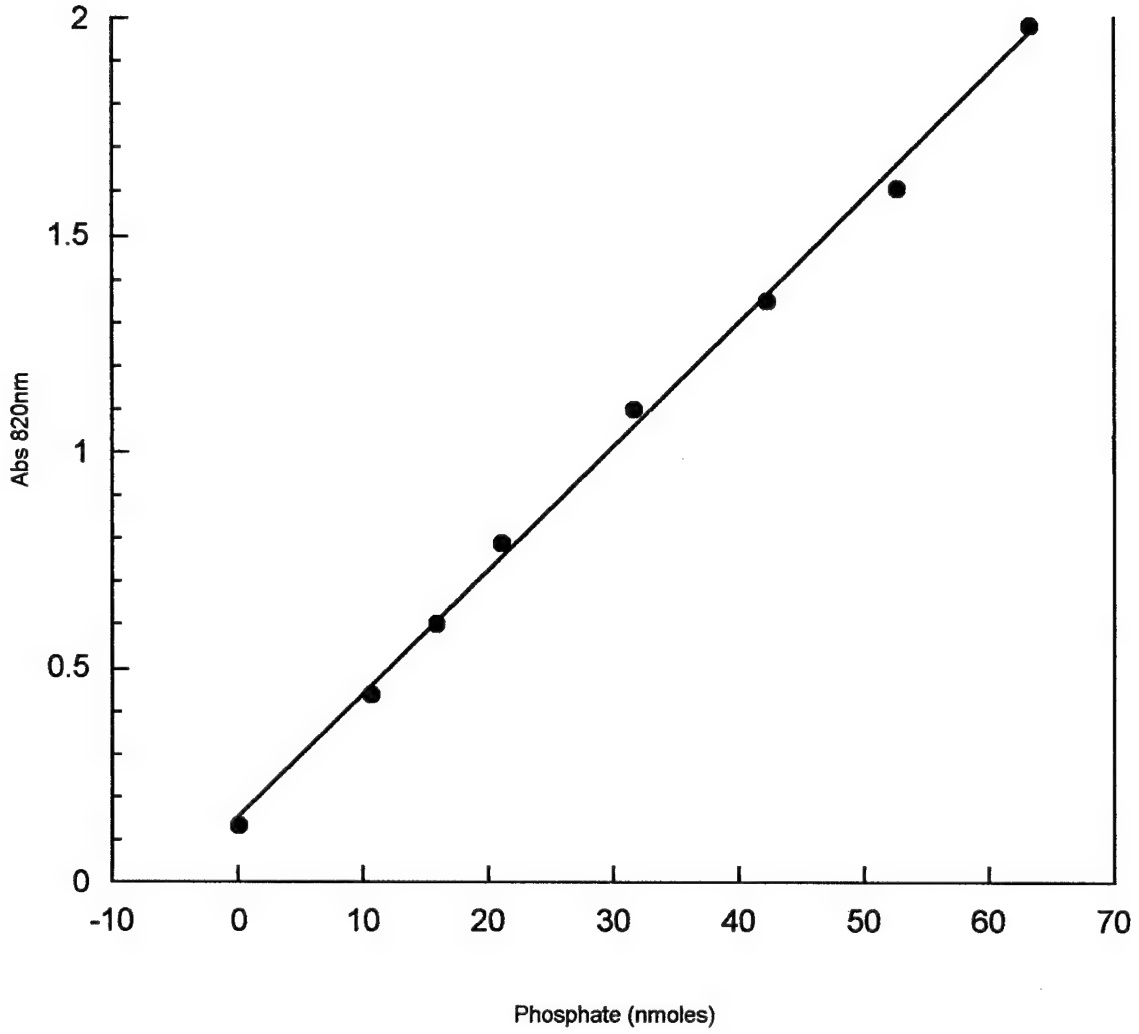

Figure 3.2-1 Standard curve for total phosphate determination

mounted through the loop-gap resonator so that the lower end of the capillary could be immersed into the PC/proxyl-PIP_2 vesicle suspension. A stainless steel plunger was used to draw solution into the capillary so that its EPR spectra could be recorded. This set-up allowed peptides and other molecules to be titrated into the lipid suspension without sample removal and re-tuning of the resonator. (Figure 3.2-2).

Titrations into the PC/PIP_2-sl vesicles were done with neomycin, native MARCKS (151-175), pentalysine, SCAMP (230-240), and the isolated native PLC-δ_1 PH domain.

3.2.7 Proxyl-PIP_2 power saturation

Power saturation experiments were performed on both proxyl-PIP_2 within 20 mM PC vesicles and proxyl-PIP_2 within PC:PS (3:1) vesicles. For power saturation of the proxyl-PIP_2 within PC vesicles, 20 mM NiAcAc was used as the polar paramagnetic relaxation agent. For power saturation of the PIP_2-sl within PC/PS vesicles, 20 mM NiEDDA was used as the polar paramagnetic relaxation agent. The choice of whether to use either NiAcAc or NiEDDA as the polar relaxation agent was determined by if the system to be analyzed contained PS lipid. While both NiAcAc and NiEDDA partition to some extent into the lipid bilayer, the partitioning of NiEDDA seems to be dependent on negative lipid concentration (in-house communication). To ensure a substantial polar relaxation gradient in neutral lipid, NiAcAc was used instead of NiEDDA. In addition, Φ calibration curves for NiAcAc in PC lipid and NiEDDA in PC/PS lipid are well established.

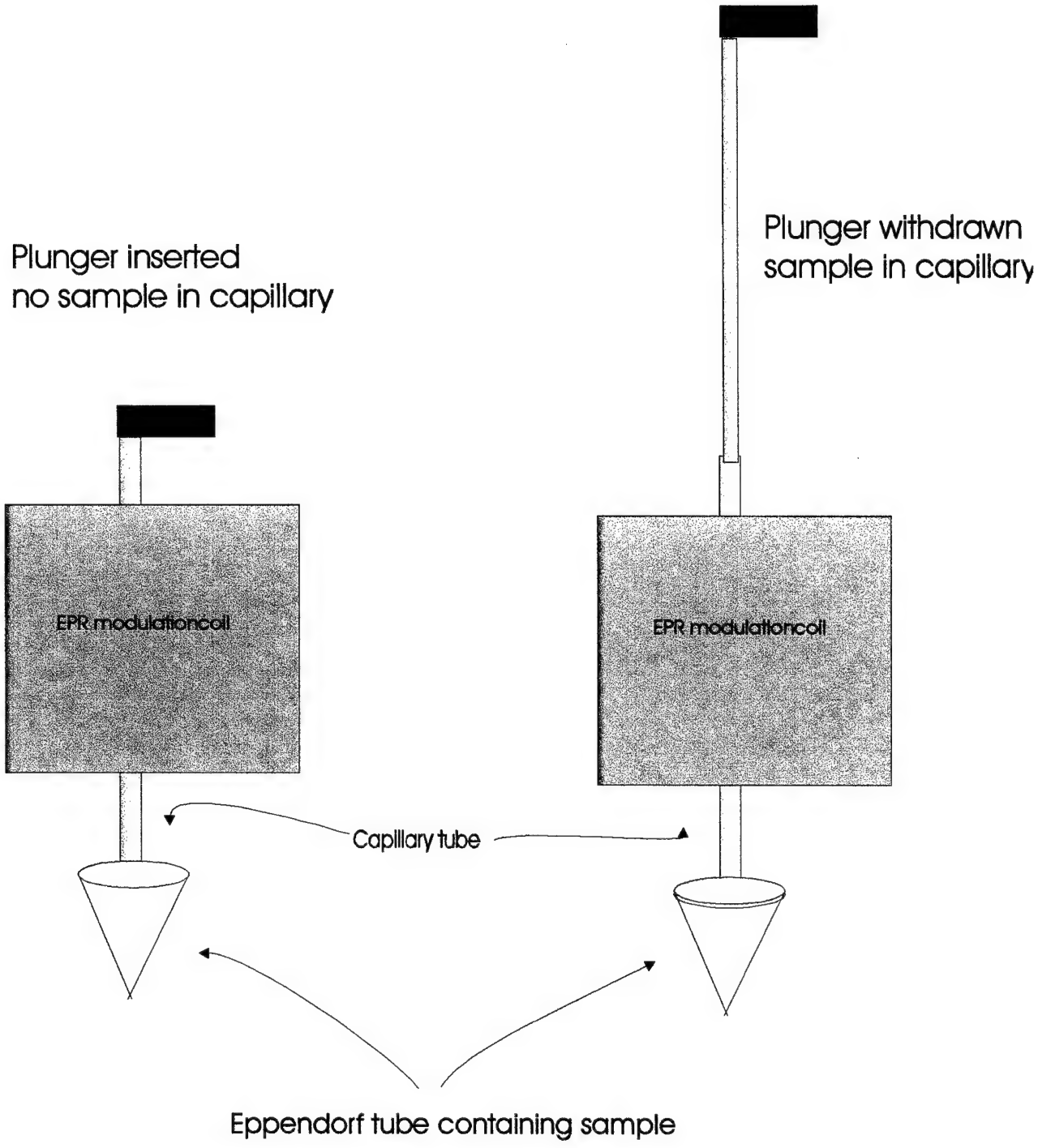

Figure 3.2-2 EPR titration experimental set-up (components not to scale)

3.2.8 Spin-labeled MARCKS peptide experiments

The binding of 40 μM spin-labeled MARCKS cysteine derivatives to vesicles containing either 40 mM PC, 40 mM PC/10%PS or 40 mM PC/1.5%PIP_2 was evaluated by comparing the EPR spectra obtained in all three vesicle environments.

The power saturation experiments with the single spin-labeled MARCKS (151-175) peptides were performed in lipid vesicles containing 40 mM PC 2% PIP_2.

3.2.9 Low temperature EPR

For the frozen state EPR data, the samples were loaded in capillary tubes and placed in the loop gap resonator. The resonator was surrounded with a low temperature dewar which in turn was fitted to a connecting dewar . Nitrogen was passed through tubing immersed in liquid nitrogen. This cooled nitrogen gas passed through the connecting dewar into the low temperature dewar to flow up and around the resonator lowering the temperature of the sample to approximately -40C (Figure 3.2-3).

Low temperature EPR data was acquired of the proxyl-PIP_2 in 20 mM PC vesicles and 20 mM PC 3% PIP_2 1% proxyl-PIP_2 both in presence and absence of the MARCKS(151-175) peptide.

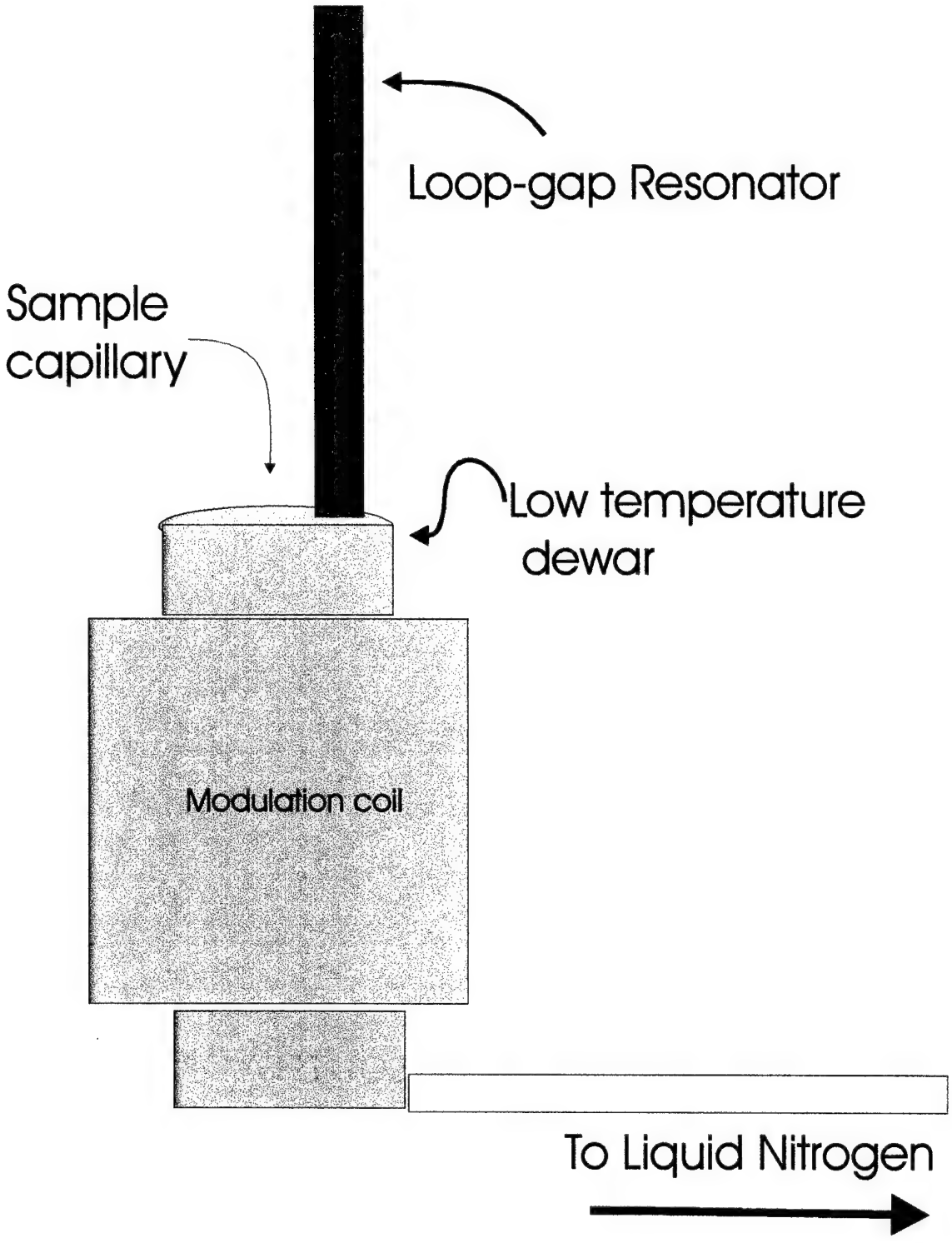

Figure 3.2-3 Low temperature EPR experimental set-up

Chapter 4 Results and Discussion

4.1 Results

4.1.1 Characteristics of proxyl-PIP_2 probe

The proxyl-PIP_2 dissolves readily in chloroform and as seen in Figure 4.1-1 the EPR spectrum indicates strong spin exchange. The center of the peaks have a sharp Lorenzian component while the spectrum as a whole has been broadened. Strong spin exchange is a characteristic of a molecule forming inverted micelles, an expected behavior of a charged lipid in an organic solvent. An EPR spectrum of aqueously dissolved proxyl-PIP_2 was not obtainable at room temperature. PIP_2 is known to form micelles in aqueous solution at nM concentrations, and proxyl-PIP_2 is also expected to form micelles. Formation of micelles by the proxyl-PIP_2 would place the proxyl labels directly next to each other. No discernible spectrum would be seen because resulting Heisenburg exchange between spins would extremely broaden the signal. Even at concentrations as low as 5 μM of proxyl-PIP_2, no EPR signal was seen, indicating that the critical micelle concentration (CMC) of the proxyl-PIP_2 is comparable to the nM concentrations of PIP_2. Upon addition of PC lipid vesicles to a thin dried film of proxyl-PIP_2, the EPR spectrum shown in Figure 4.1-2 was observed. The EPR spectrum indicates the proxyl-PIP_2 is incorporated into the lipid vesicles as a monomer and the label is undergoing fairly rapid, isotropic motion.

Power saturation data of the proxyl-PIP_2 in PC vesicles and PC/PS vesicles is shown in Figure 4.1-3 and Table 4.1-1. In PC vesicles the Φ value, or depth parameter for the proxyl-

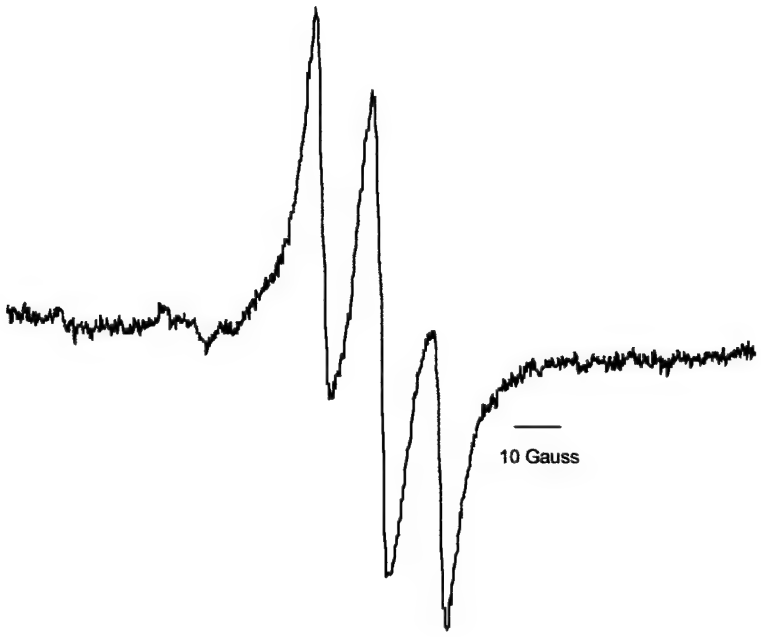

Figure 4.1-1 EPR spectrum of 200μM proxyl-PIP_2 dissolved in chloroform

PIP_2 was Φ= -0.77 using 20mM NiAcAc as the polar relaxing agent. From a reference calibration curve for PC bilayers this Φ value indicates the proxyl-label sits at a location of 3±2 Å below the level of the lipid phosphate (Altenbach et al., 1994). In PC/PS vesicles the Φ value for the proxyl-PIP_2 was Φ=0.46 using 20mM NiEDDA. A recent calibration curve for PC/PS bilayers with this Φ value places the label at a position 6±2 Å below the level of the lipid phosphate (Victor and Cafiso, 2001). Both power saturation experiments indicate that the proxyl label resides a few Å below the lipid phosphate within the bilayer. If the acyl chain with the proxyl spin label were fully extended, this would place the label about 10 Å deeper than the Φ values indicate.

Full incorporation of the total added amount of proxyl-PIP_2 to vesicles was verified through double integration of the EPR spectrum in Figure 4.1-2. Furthermore, because of the -3 net charge at neutral pH of the PIP_2 molecule, transmembrane migration of the molecule is energetically unfavorable. Therefore, the total amount of incorporated proxyl-PIP_2 is located on the external surface of the lipid vesicles and is available for interaction with externally added binding molecules.

4.1.2 Binding of proxyl-PIP_2 to

4.1.2.1 Neomycin

The strong 1:1 binding of neomycin to PIP_2 is well established (Arbuzova et al., 2000a). Figure 4.1-4 shows the EPR spectrum of proxyl-PIP_2 in PC vesicles in the presence and absence of neomycin. The EPR spectrum with neomycin exhibits broadening which corresponds to an increase in rotational correlation time of about 25%.

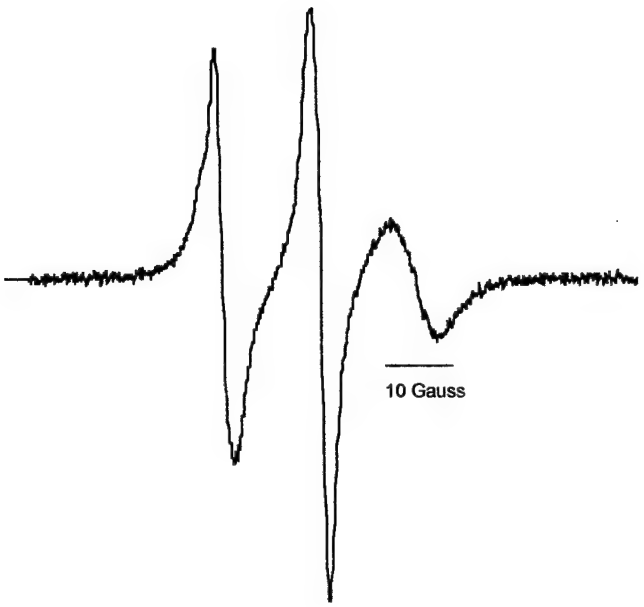

Figure 4.1-2 EPR spectrum of 100 μM proxyl-PIP_2 incorporated into PC vesicles. *It may be noted that in some of the following spectra containing proxyl-PIP_2 there is a small shoulder on the low field peak. This shoulder is the result of imperfect subtraction of a minimal amount of free proxyl spin label contaminant and can be disregarded as it does not effect the interpretation of the data.

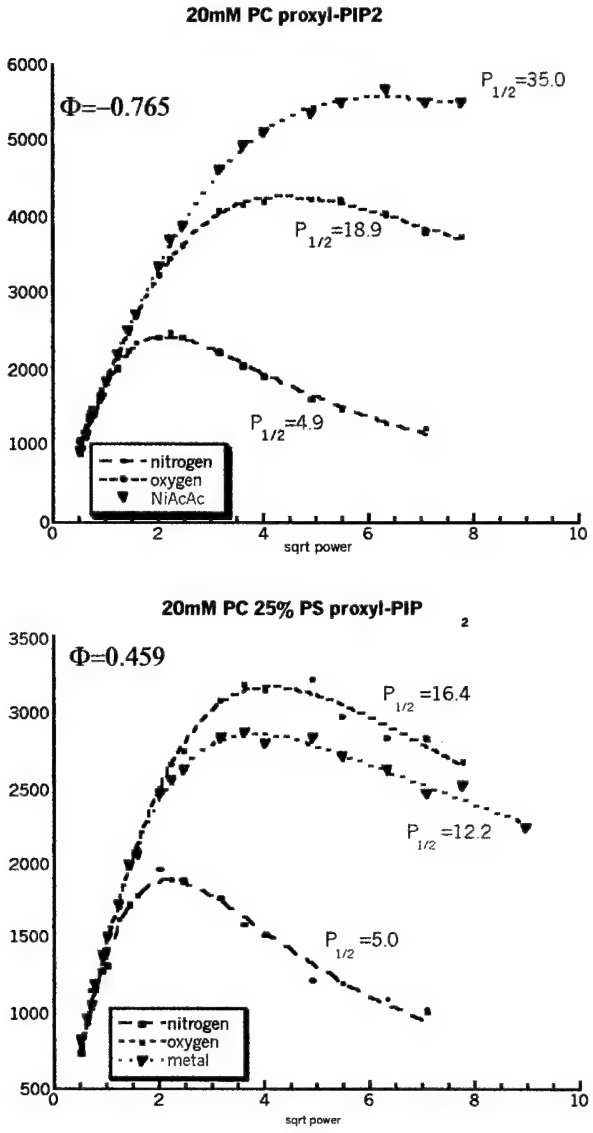

Figure 4.1-3 Power saturation data of proxyl-PIP_2 in PC and PC:PS vesicles. For power saturation of proxyl-PIP_2 in PC vesicles 20 mM NiAcAc was used the polar paramagnetic relaxing agent, for PC:PS 20 mM NiEDDa was used as the polar paramagnetic relaxation agent

Power Saturation of 50 μM proxyl-PIP_2 in:	**Φ value obtained**	**Depth within bilayer**
20 mM PC	**-0.77**	**3±2Å**
20 mM PC 25% PS	**0.46**	**6±2Å**

Table 4.1-1 Φ values and depth parameters of proxyl-PIP_2 obtained from EPR spectrum power saturation data

To further characterize the interaction of the proxyl-PIP_2 with neomycin, an EPR titration experiment was performed (see Methods 3.2.6). Figure 4.1-5 shows the plot of the neomycin concentration versus the first derivative EPR central line amplitudes. These data points were fit (see Section 2.2.3) assuming 1:1 binding of neomycin to PIP_2. For this fit, both K_a and A_b were taken as adjustable parameters. As seen in Figure 4.1-5 the fit of the data is quite good and gives a K_a value of approximately 3×10^5 M^{-1}.

4.1.2.2 PLCδ_1 PH domain

The PLC δ_1 PH domain is another well established PIP_2 binding molecule. PLC δ_1 PH domain and PIP_2 form a high affinity 1:1 complex. Figure 4.1-6 shows the EPR spectrum of proxyl-PIP_2 in PC vesicles in the presence and absence of the PLC δ_1 PH domain . Complementary to the results for neomycin, the EPR spectrum in the presence of the PLC δ_1 PH domain is broadened and indicates an increase in rotation correlation time of about 25%.

The EPR data shows that it was possible to fully saturate the proxyl-PIP_2 with PLC δ_1 PH domain protein and to witness the decrease in motion the protein's binding had on the spin label. However, attempts at titrating the proxyl-PIP_2 with PLC δ_1 PH domain were inconclusive (data not shown). Numerous attempts to calculate PLC δ_1 PH protein concentration were made using both the published extinction coefficient and a modified Bradford assay. The precise concentration of the PLC δ_1 PH domain protein purified was unable to be reproducibly determined. Therefore, it was not possible to perform an accurate titration of the proxyl-PIP_2 with PLC δ_1 PH domain.

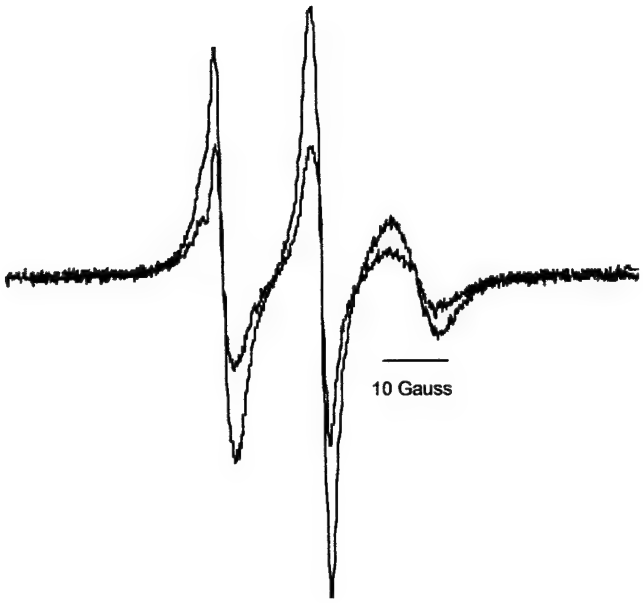

Figure 4.1-4 EPR spectra of proxyl-PIP_2 in absence (blue) and presence (red) of neomycin

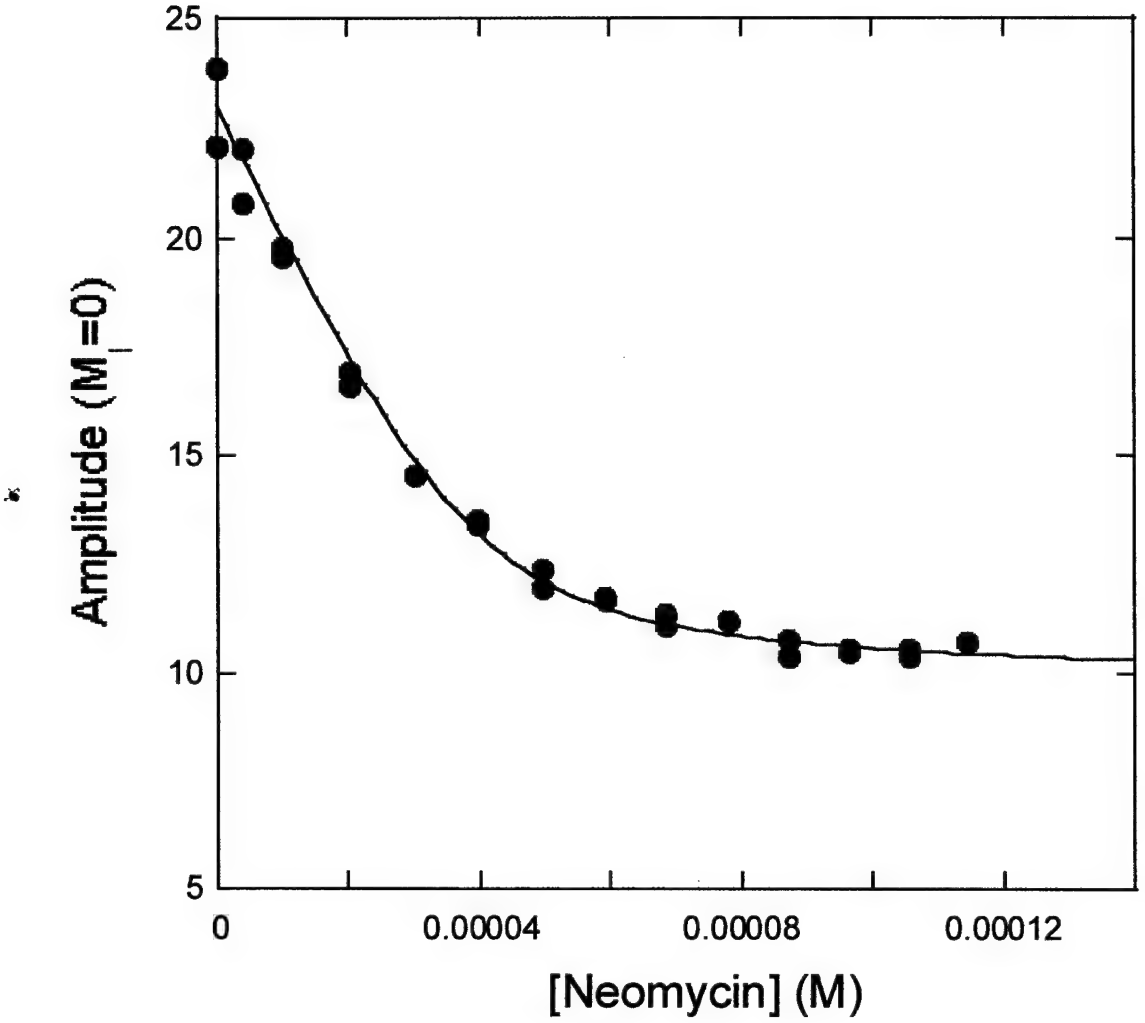

Figure 4.1-5 EPR titration of proxyl-PIP_2 with neomycin. Data (●) represent two independent titrations. Solid line represents non-linear best fit assuming 1:1 binding stoicheometry

4.1.2.3 Pentalysine

Pentalysine is a small basic peptide with a net charge of +5 that is known to bind to acidic lipid, including PIP_2. Shown in Figure 4.1-7 are EPR spectrum of proxyl-PIP_2 in presence and absence of pentalysine. The EPR spectrum of proxyl-PIP_2 in the presence of pentalysine, is broadened considerably less than in the presence of the other molecules studied. Pentalysine is known to bind through only electrostatics above the head group of an acidic lipid molecule. Although, this slows down the rotation correlation time of the proxyl-PIP_2 molecule slightly, it is minimal compared to the decreases seen in the presence of the neomycin and the PH domain.

The evidence for the weak binding of the pentalysine to the proxyl-PIP_2 is further supported by the titration of the proxyl-PIP_2 with pentalysine as shown in Figure 4.1-8. Unlike, the titration data for neomycin and the PH domain, which quickly reach a minimum value and stay there, the pentalysine titration data does not reach a minimum but continues to steadily decrease. This continued decrease indicates that as even very high concentrations of pentalysine are reached, the motion of the proxyl-PIP_2 has not been fully restricted. If a weak interaction exists between the two molecules, at very high concentrations of pentalysine the rotational or diffusive motion of the proxyl-PIP_2 would be expected to slow. However, without direct steric constraints placed on the proxyl-PIP_2 by a strong interaction with pentalysine, the central peak to peak amplitude would continue to decrease, as seen in the pentalysine titration data.

4.1.2.4 SCAMP

Shown in Figure 4.1-9 are the EPR spectrum of proxyl-PIP_2 in the presence and absence of the SCAMP peptide. The broadening of the EPR spectrum indicates a decrease in the dynamics of the proxyl spin-label. This broadening is consistent with data that supports SCAMP binds to PIP_2. However, the titration data shown in Figure 4.1-10 indicate that the binding between the two molecules must be of a lower affinity that that seen for neomycin or the PH domain. The central line peak to peak amplitude does not reach and plateau at a minimum. As with pentalysine, the interaction of SCAMP with proxyl-PIP_2 seems to involve weak binding.

4.1.3 Interaction between proxyl-PIP_2 and MARCKS

Shown in Figure 4.1-11 are the EPR spectrum of the proxyl-PIP_2 in PC vesicles in the presence and absence of MARCKS (151-175) peptide. MARCKS has a high affinity for membranes containing PIP_2, and as depicted in Figure 4.1-10 in the EPR spectrum is broadened in the presence of MARCKS (151-175). The broadening of the proxyl-PIP_2 EPR spectrum, in this case is greater than that observed upon addition of either neomycin or the PLC δ_1 PH domain to the proxyl-PIP_2 containing vesicles (Figure 4.1-12).

In order to examine whether the increased broadening of the EPR spectrum arises from spin-spin interactions from the close proximity of multiple proxyl-PIP_2 bound to MARCKS, a dilution experiment was performed. Dilution of the proxyl-PIP_2 with unlabeled PIP_2 reduces/eliminates dipolar interactions between spin-labels when bound to MARCKS by replacing each proxyl-PIP_2's three proxyl-PIP_2 neighbors with three unlabeled PIP_2. Lipid vesicles were made that contained 3:1 unlabeled PIP_2 to proxyl-

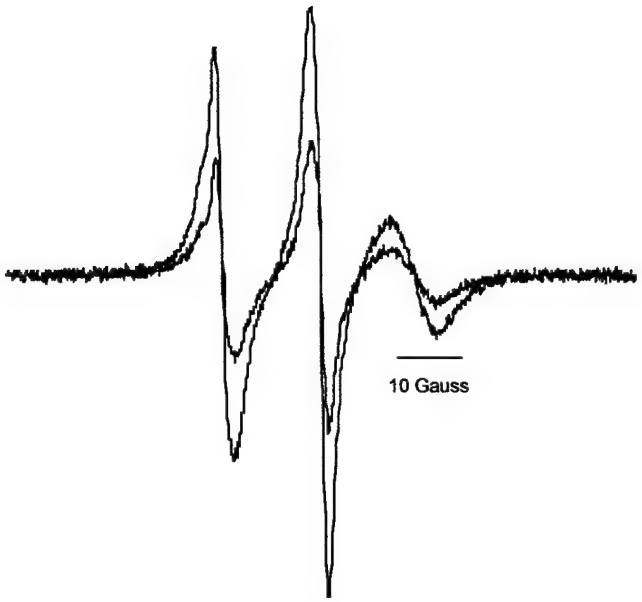

Figure 4.1-6 EPR spectrum of proxyl-PIP_2 in absence (blue) and presence of PLC δ1 PH domain (red)

Figure 4.1-7 EPR spectrum of proxyl-PIP_2 in absence (dashed line) and presence (solid line) 0f 200μM pentalysine

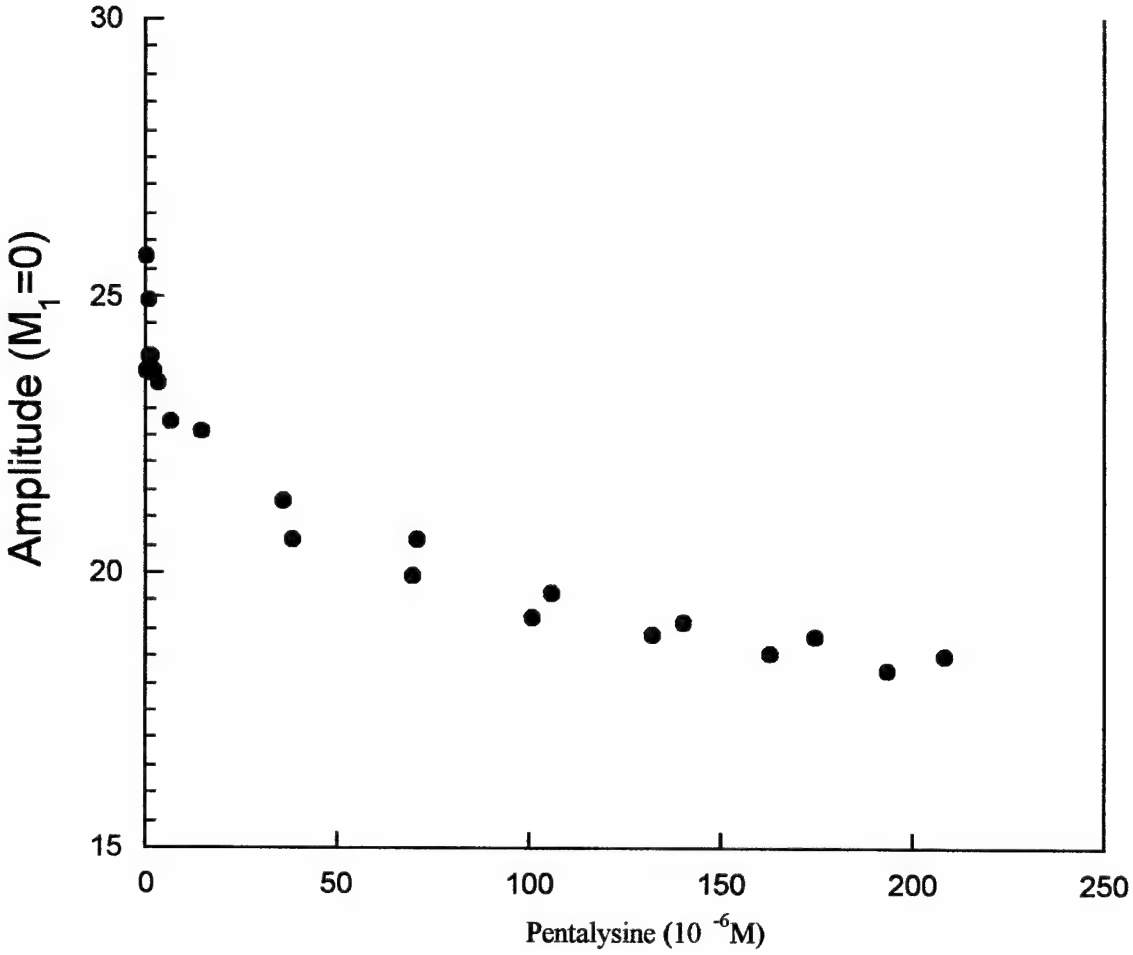

Figure 4.1-8 EPR titration of proxyl-PIP_2 with pentalysine. Data (●) are from two independent titration experiments

labeled PIP_2. Figure 4.1-13 shows undiluted proxyl-PIP_2 vesicles in presence and absence of MARCKS (151-175) as well as diluted proxyl-PIP_2 vesicles in presence and absence of MARCKS (151-175). When the spin labeled lipid is diluted the proxyl-PIP_2 EPR spectrum is still broadened, however, the effect is significantly less than in the undiluted vesicles. This is strong evidence that MARCKS (151-175) binds to multiple PIP_2s.

To further investigate possible spin-spin interactions between closely situated proxyl-PIP_2 bound to MARCKS (151-175) these samples in presence and absence of MARCKS were examined using low temperature EPR spectroscopy. Figure 4.1-14 shows the two sets of low-temperature spectra. For the diluted proxyl-PIP_2 spectrum in presence and absence of MARCKS(151-175) there is no significant difference in spectrum. For the undiluted proxyl-PIP_2 spectrum in presence and absence of MARCKS (151-175), there is a significant difference. The d_1/d ratio (see Section 2.2.4) for the proxyl-PIP_2 in absence of MARCKS is approximately 0.41 while the d_1/d ratio for the proxyl-PIP_2 in the presence of the peptide is approximately 0.39. A value of >0.4 is indicative that the two spin-labels are at a distance of closer than 25 Å . The value for the d_1/d ratio of the proxyl-PIP_2 bound to MARCKS (151-175) indicates that the proxyl-PIP_2s are separated by a distance of approximately 18 to 22 Å .

An EPR titration experiment was done to further characterize the interaction of the proxyl-PIP_2 with the MARCKS (151-175) peptide. Seen in Figure 4.1-15 is the data from this titration experiment. As with the neomycin, the titration of the proxyl-PIP_2 with MARCKS (151-175) was fit using Equation 2-19 to estimate the fraction of bound proxyl-PIP_2. If 1:1 binding of the proxyl-PIP_2 with the peptide is assumed, the data

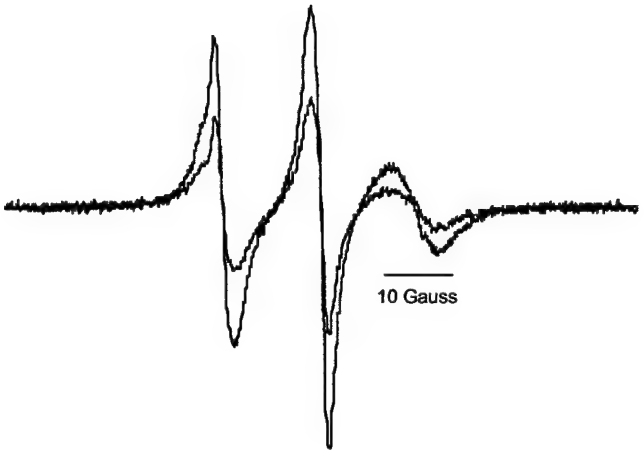

Figure 4.1-9 EPR spectrum of proxyl-PIP_2 in absence (blue) and presence (red) of 200μM SCAMP peptide

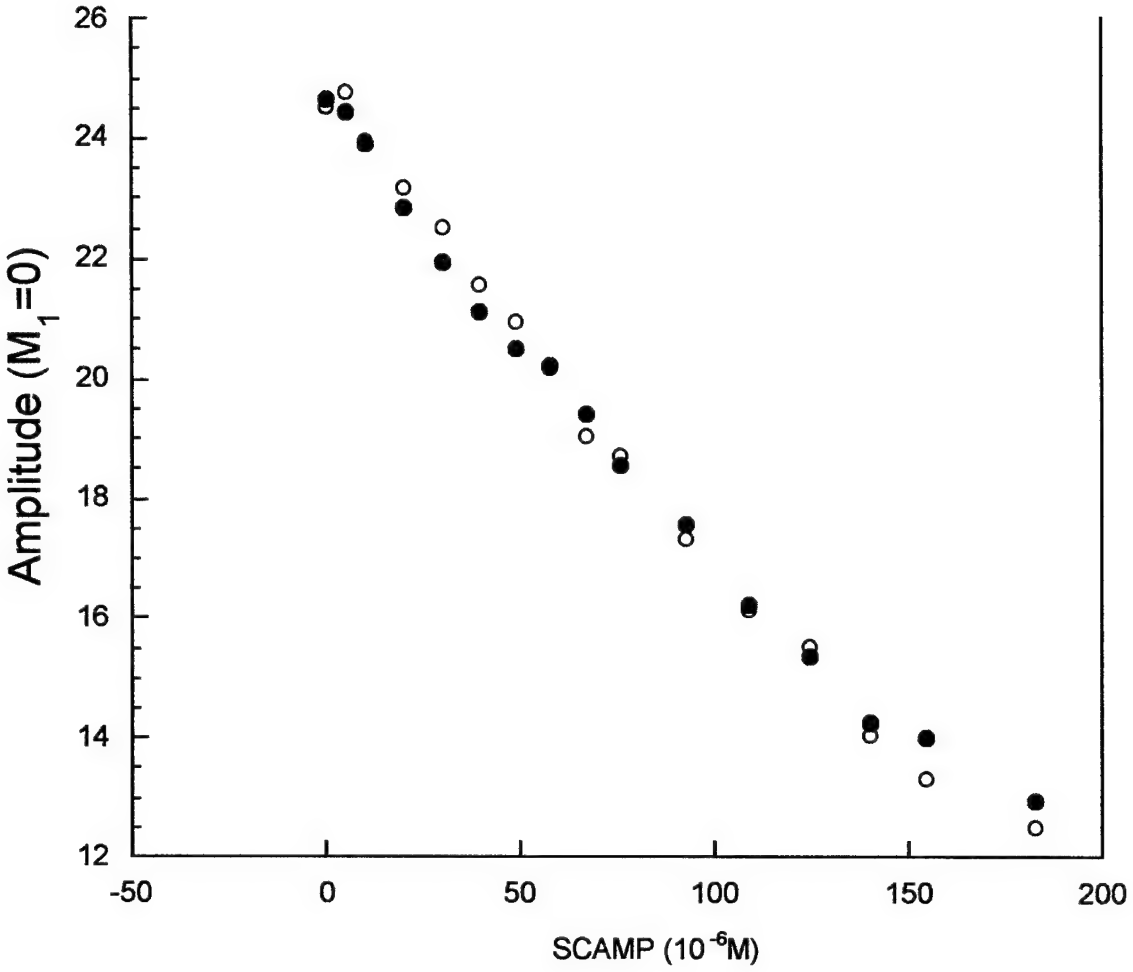

Figure 4.1-10 EPR titration of proxyl-PIP_2 with SCAMP peptide. Data (●) are from two independent titration experiments

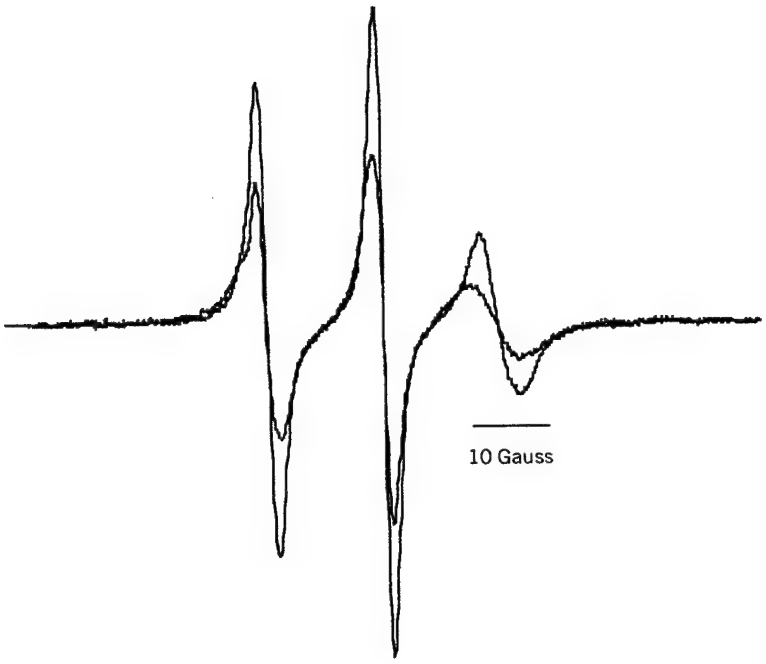

Figure 4.1-11 EPR spectrum of proxyl-PIP_2 in absence (blue) and presence (red) 100uM MARCKS (151-175) peptide

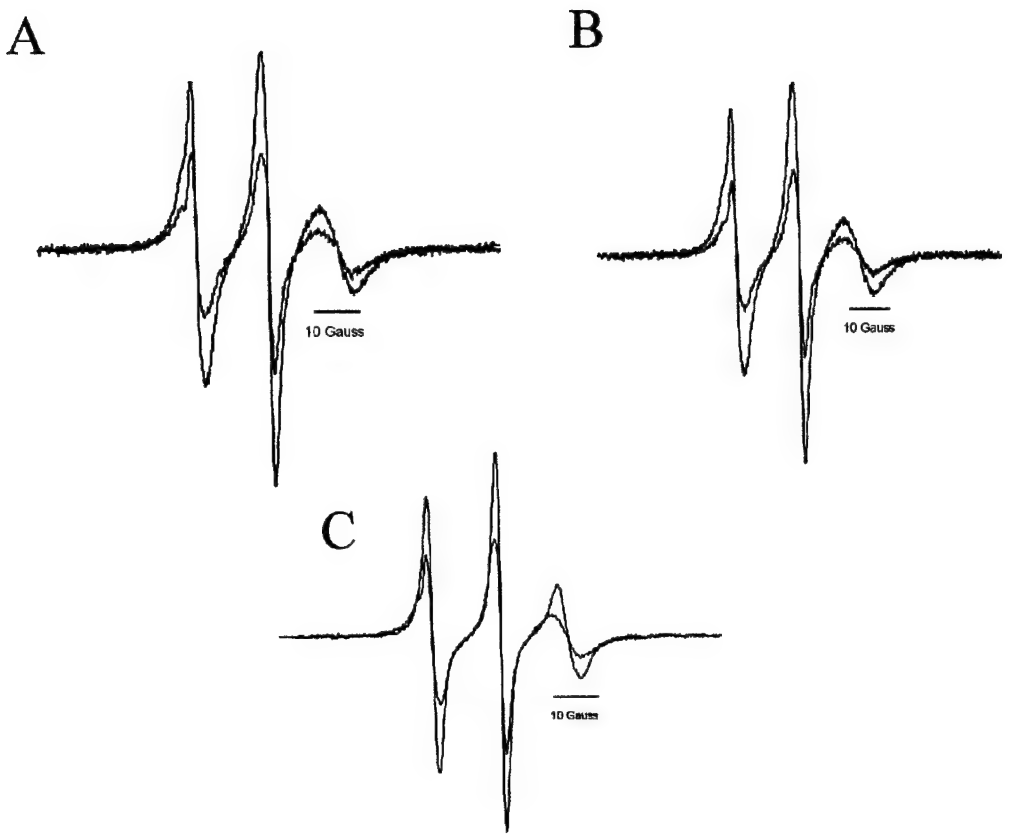

Figure 4.1-12 EPR spectrum of proxyl-PIP_2 (blue) in presence of A) neomycin (red) B) PLC δ_1 PH domain (red) and C) MARCKS (151-175) peptide (red). For each of the PIP_2 binding molecules the concentration added was sufficient to fully bind the PIP_2

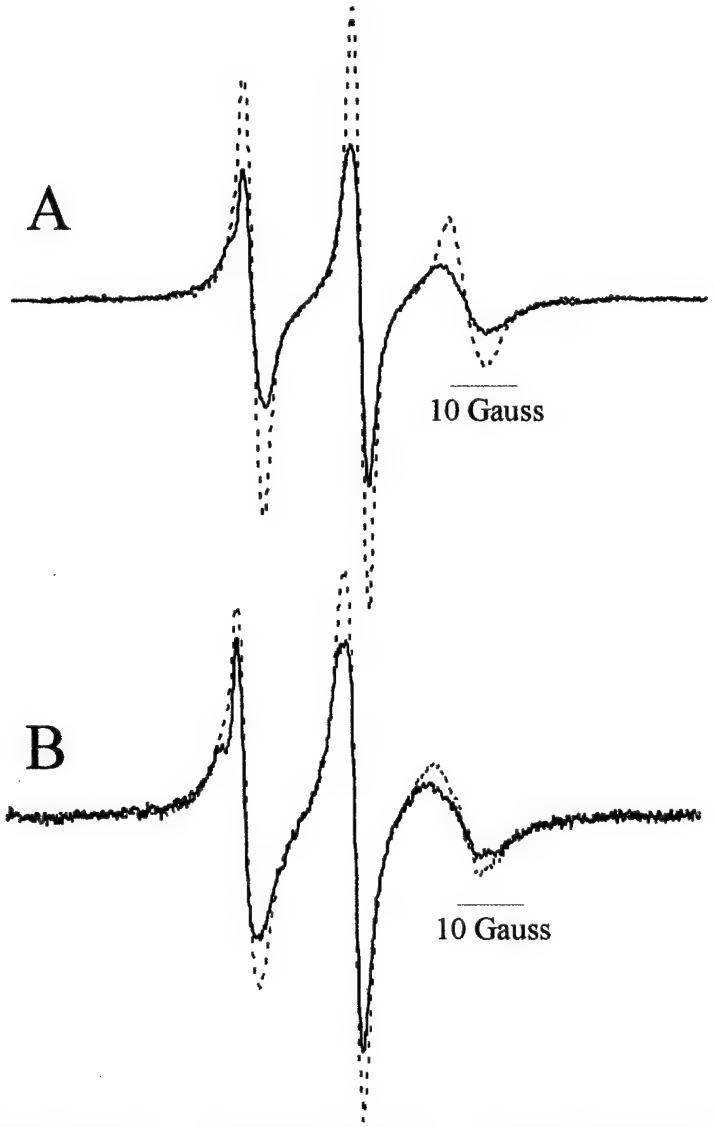

Figure 4.1-13 EPR spectrum of proxyl-PIP_2 in A) undiluted (blue) and B) 3:1 unlabeled PIP_2 diluted (red) vesicles in the absence (dashed line) and presence (solid line) of MARCKS (151-175) peptide

cannot be fit, regardless of how the affinity constant parameter is adjusted. This fit is shown in Figure 4.1-15 as the solid line. However, by allowing n and K_a to be adjustable parameters, the best fit shown by the dashed line is obtained. A value of n=3 gives the best fit for this data. However, any ratio of 2.5 to 3.5 proxyl-PIP_2 to MARCKS (151-175) gives an acceptable fit. The apparent partition coefficient, K_a, obtained with the best fit was 4×10^5 M^{-1}.

Power saturation of the EPR spectrum of the proxl-PIP_2 in the presence of MARCKS (151-175) was performed, the data is shown in Figure 4.1-16. The Φ value obtained was 0.48. Using the same calibration curve as for the power saturation of the proxyl-PIP_2 in the absence of MARCKS (151-175), this Φ value indicates a depth of approximately 6Å below the lipid phosphate, only slightly deeper than in the absence of the peptide.

4.1.4 Spin labeled MARCKS peptide interactions with PIP_2

4.1.4.1 Comparisons of EPR spectrum of spin-labeled MARCKS peptides in buffer and three different lipid vesicles

The position and structure of the MARCKS (151-175) peptide was examined when bound to PIP_2 containing vesicles. Figures 4.1-17, 4.1-18 and 4.1-19 show EPR spectrum of spin-labeled MARCKS cysteine derivatives dissolved aqueously, and in the presence of PC, PC:PS and PC:PIP_2 vesicles. MARCKS (151-175) is known to dissolve aqueously and for each of the EPR spectra of the spin-labeled peptides in buffer, the lineshape is characteristic of monomeric species with a fast rotation correlation time. Likewise, the EPR spectrum of the spin-labeled peptides in the presence of PC containing

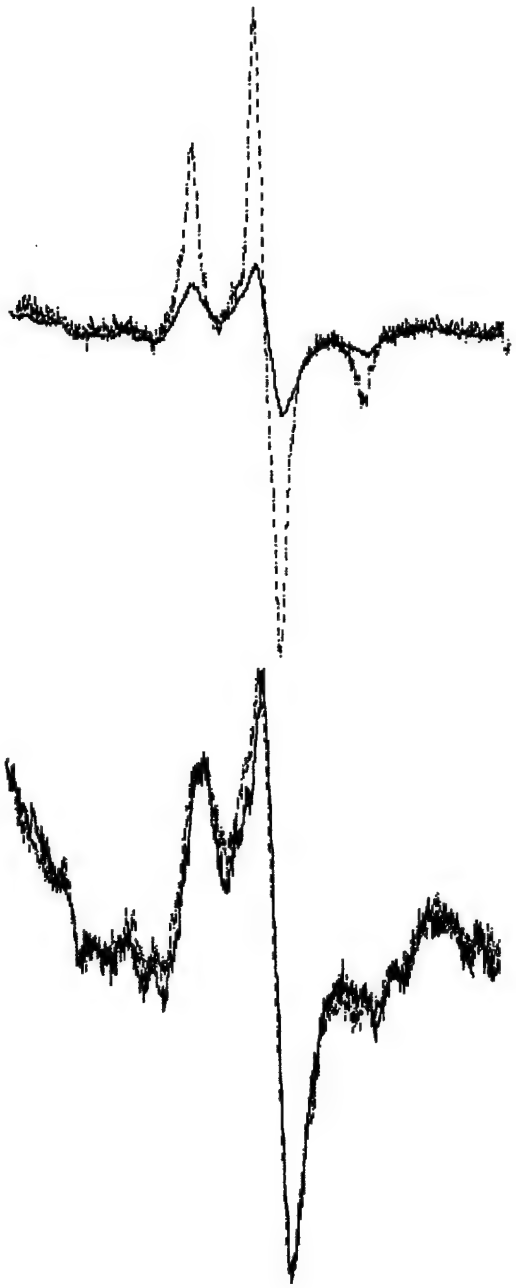

Figure 4.1-14 Low temperature EPR spectra of proxyl-PIP_2 undiluted (blue) and 3:1 unlabeled PIP_2 diluted (red) vesicles in the absence (dashed line) and presence (solid line) of MARCKS (151-175) peptide (total scan width 200 Gauss)

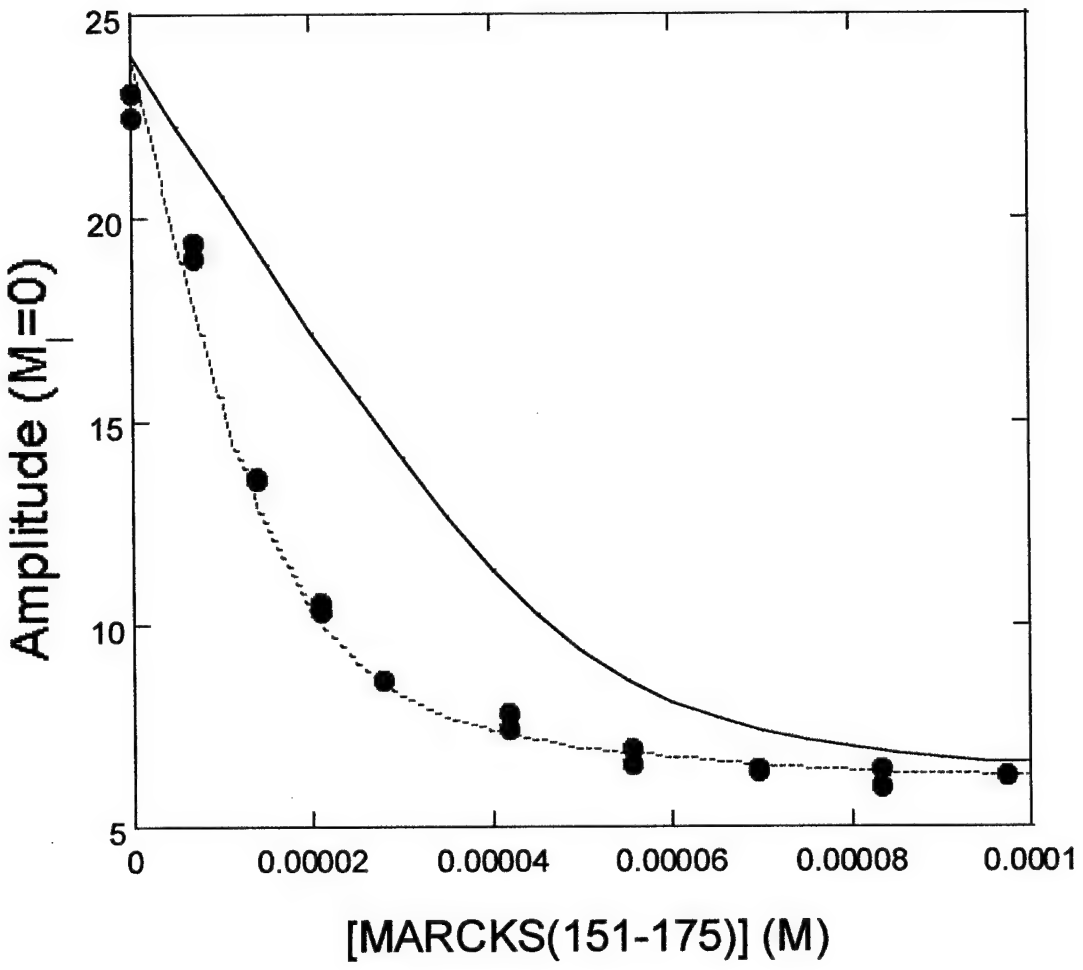

Figure 4.1-15 EPR titration of proxyl-PIP_2 with MARCKS (151-175) peptide. Data (●) are from two independent titration experiments. Solid line is a non-linear least squares fit assuming 1:1 binding of proxy-PIP_2 and peptide. Dashed line is a non-linear least squares fit that yields a binding stoicheometry of 3:1 proxyl-PIP_2 and peptide.

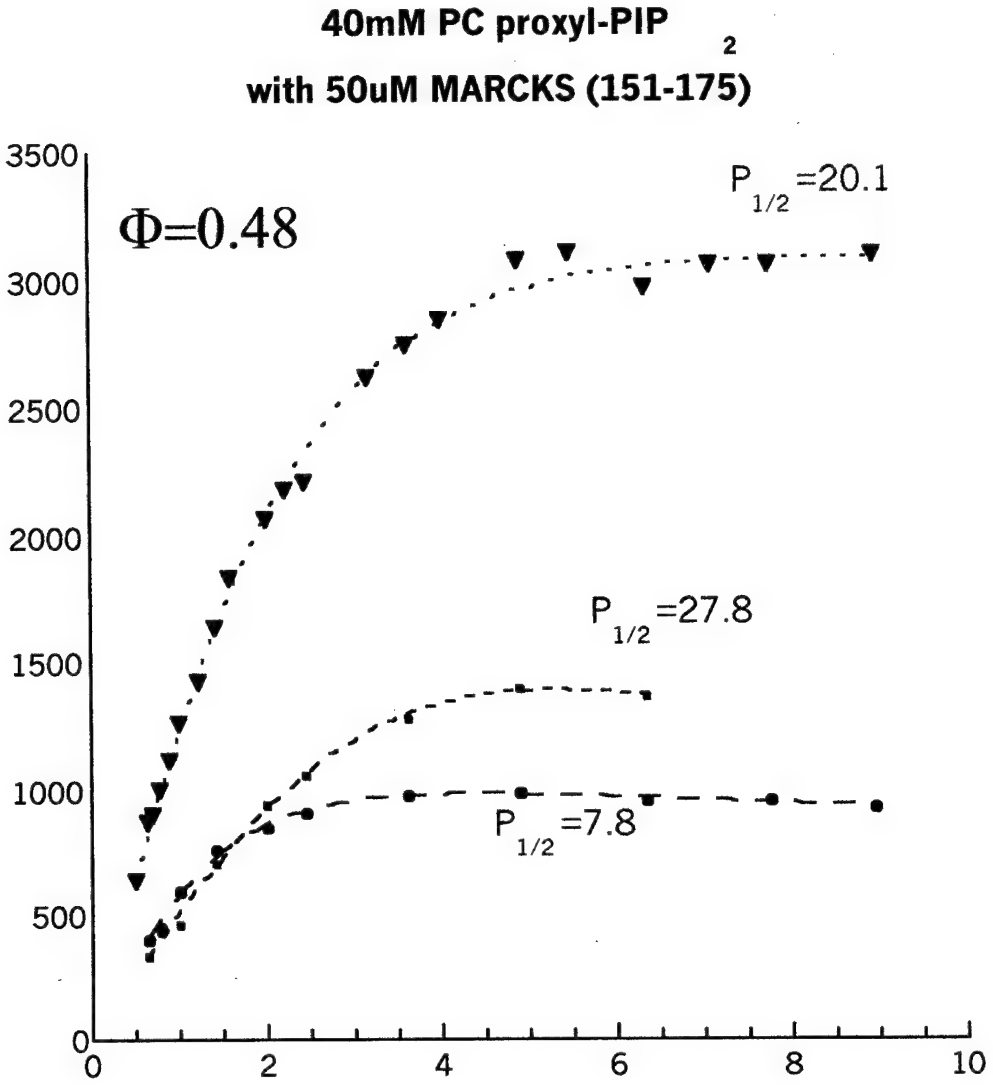

Figure 4.1-16 Power saturation data of proxyl-PIP_2 in presence of MARCKS (151-175). For Power saturation, sufficient peptide was added to fully bind the proxyl-PIP_2

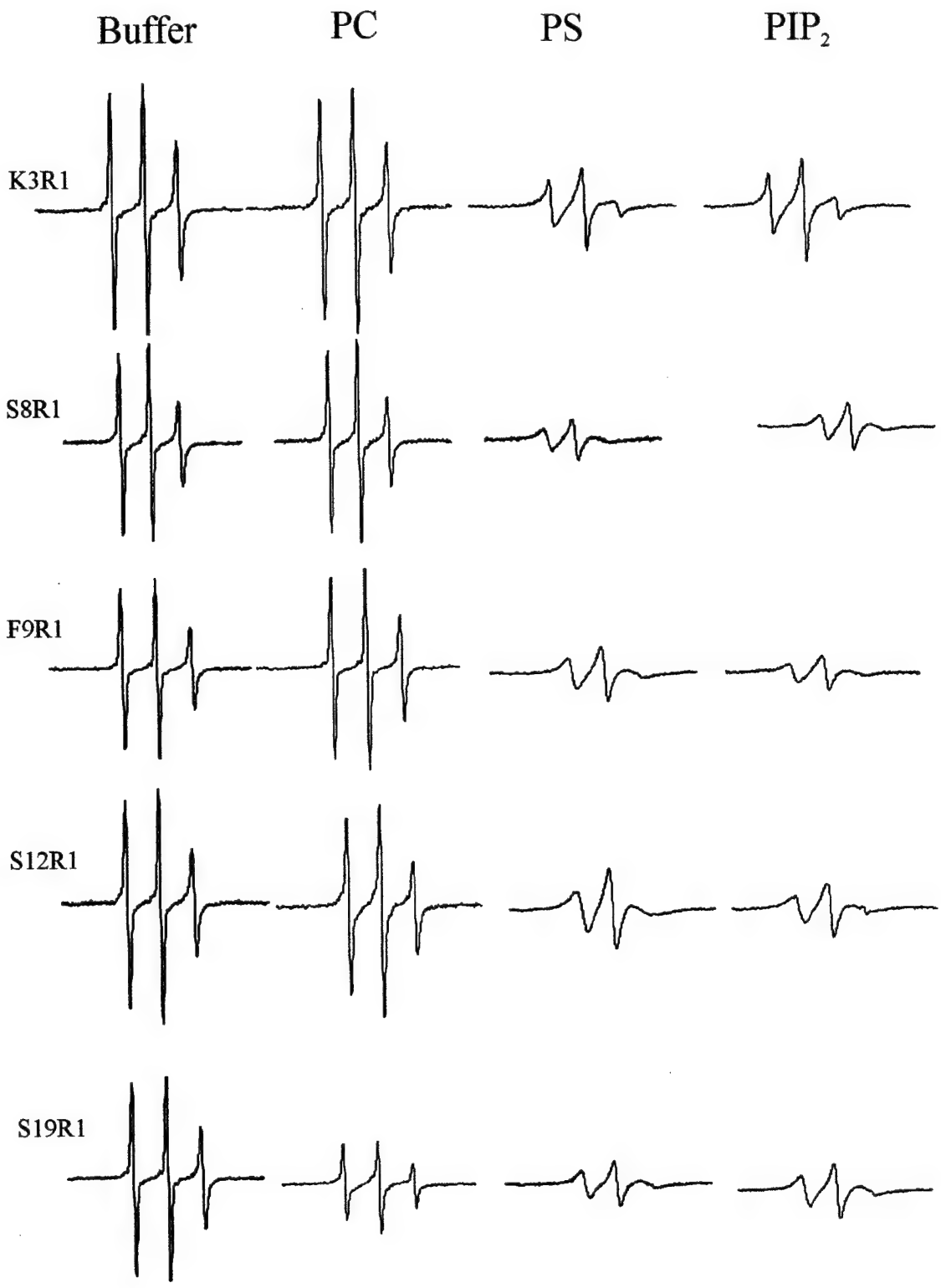

Figure 4.1-17 EPR spectra of single labeled MARCKS (151-175) cysteine derivatives in buffer (black), PC (red), PC/PS (blue) and PC/PIP_2 (green) vesicles

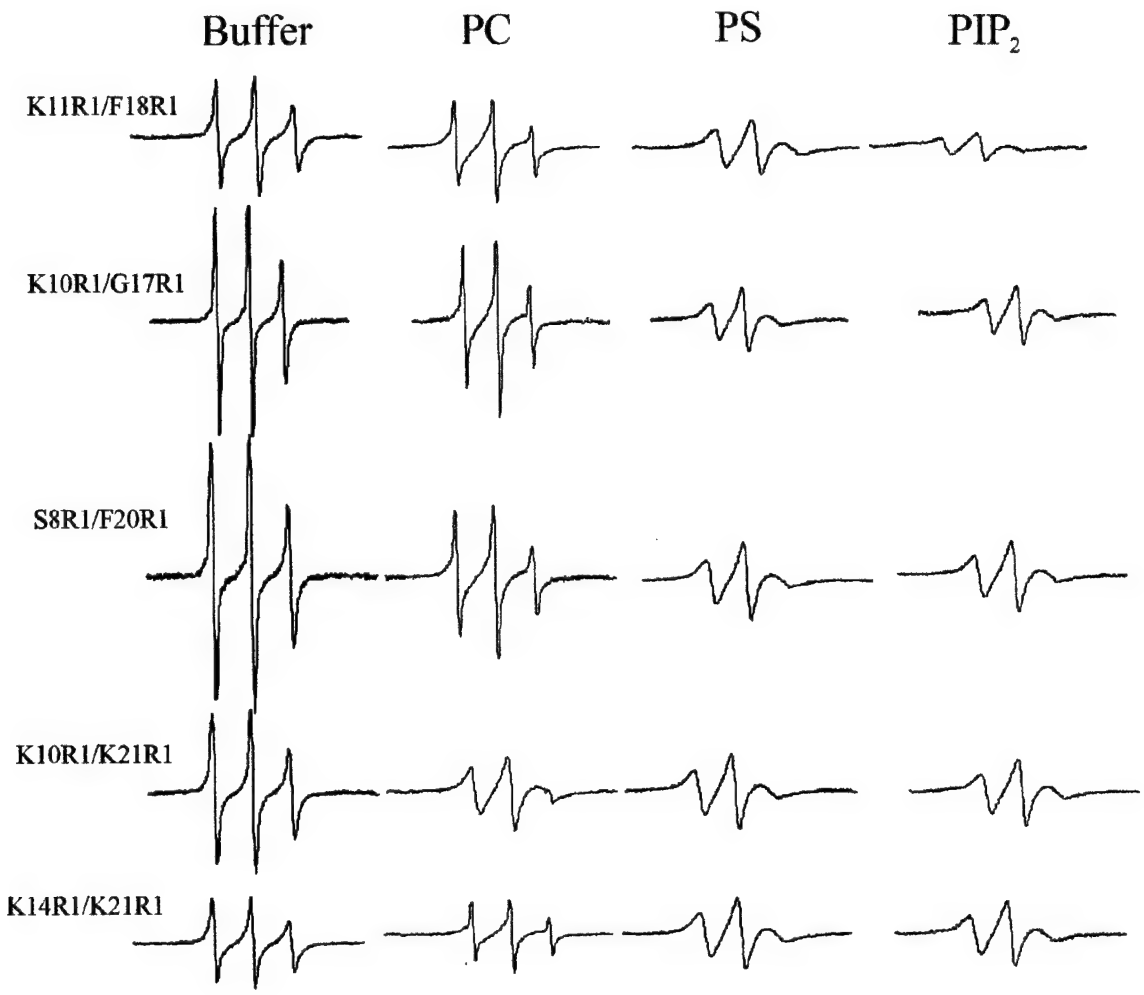

Figure 4.1-18 EPR spectra of double labeled MARCKS (151-175) cysteine derivatives in buffer (black), PC (red), PC/PS (blue) and PC/PIP_2 (green)

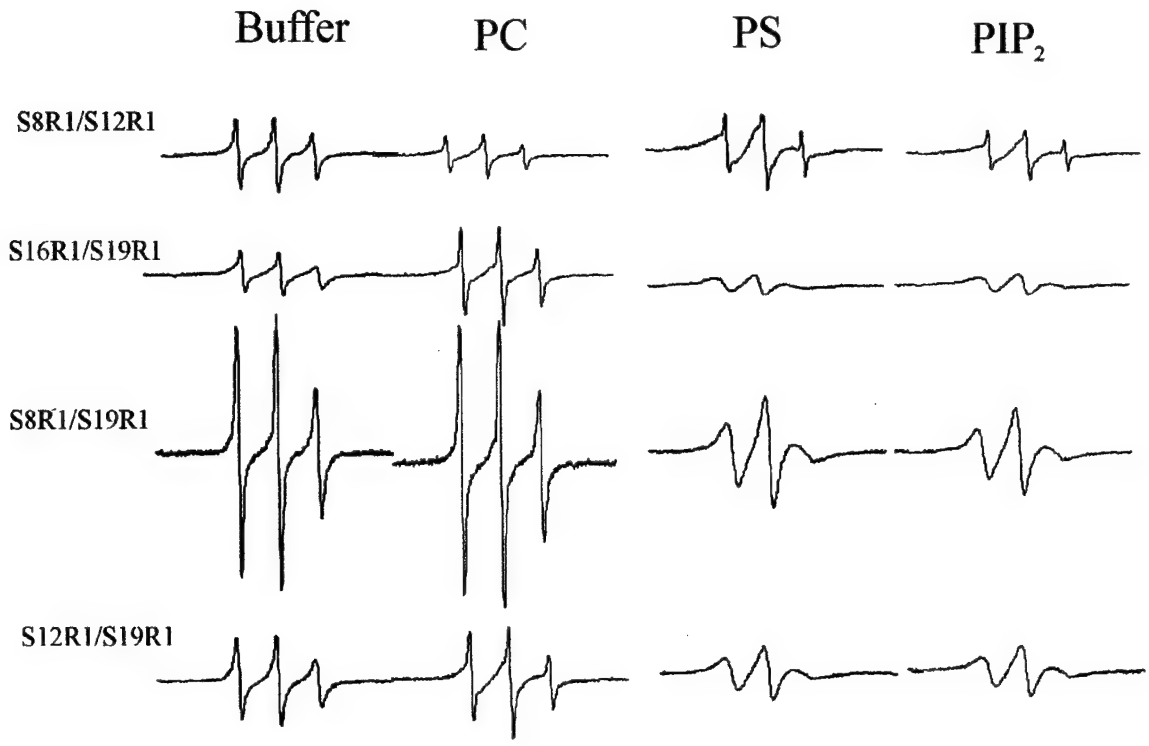

Figure 4.1-19 EPR spectra of double labeled MARCKS (151-175) cysteine derivatives that also have corresponding single-labeled MARCKS cysteine derivatives. Spectra are of peptides in buffer (black), PC (red), PC/PS (blue) and PC/PIP_2 (green)

vesicles shows a signal indicative of a relatively freely rotating molecule. MARCKS (151-175) has been shown to preferentially bind to acidic lipid thereby, the absence evidence of binding to the PC vesicles is expected. The EPR spectrum of the spin-labeled MARCKS (151-175) cysteine derivatives in the presence of PC:PS and PC:PIP_2 vesicles are essentially identical. The lineshapes of the EPR spectra of the peptides bound to lipid vesicles containing approximately the same charge ratio of either PS or PIP_2 lipid showed similar broadening but no significant differences. Table 4.1-2 shows the central linewidths for the EPR spectra of the single spin-labeled MARCKS (151-175) peptides and for five of the double spin-labeled MARCKS (151-175) peptides. MARCKS (151-175) is known to exist in the presence of PC:PS vesicles as a extended structure with the five phenylalanine residues buried in the interface and the last few N-terminal residues extending into the aqueous phase (Victor et. al, 1999). No significant differences in linewidth are seen for any of the peptides bound to PC:PIP_2 vesicles with the exception of the MARCKS K3R1 peptide. The linewidth of the EPR spectrum of the MARCKS K3R1 peptide in PC:PIP_2 vesicles is slightly less than that for the peptide bound to vesicles containing PC:PS. If there were conformational or structural differences between the MARCKS (151-175) peptides, the double labeled peptides would be sensitive to any changes resulting in differences of the two spin-label's proximity to one another. For the double-spin labeled peptides the EPR spectra show no significant difference in linewidth in the absence or presence of PIP_2.

Peptide	PC:PS	PC:PIP_2	Peptide	PC:PS	PC:PIP_2
K3R1	2.5	2.1	S8R1/F20R1	3.2	3.3
S8R1	3.2	3.4	K10R1/G17R1	3.4	3.3
F9R1	3.4	3.3	K10R1/K21R1	3.3	3.5
S12R1	3.5	3.2±0.2	S12R1/S19R1	4.0	3.9
S19R1	3.0	3.0	K14R1/K21R1	3.6	3.5
S8R1/S19R1	3.3	3.4	S16R1/S19R1	4.6	4.4

Table 4.1-2 EPR spectrum central line peak to peak splitting, ΔH (Gauss), for MARCKS (151-175) peptides in PC:PS and PC:PIP_2 . Errors in linewidths are ±0.1 Gauss unless noted

Figure 4.1-20 shows EPR spectra for two single-labeled and two double-labeled MARCKS (151-175) peptides bound to either PC:PS or PC:PIP_2. The spectra for the single-labeled peptides are unchanged regardless of whether the peptide is bound to PC:PS or PC:PIP_2. Likewise, the double labeled peptides with spin-labels at positions i,i+7 and i,i+11, show no change in EPR spectrum whether bound to PC:PS or PC:PIP_2 vesicles.

4.1.4.2 Power saturation of spin-labeled MARCKS peptides

The EPR power saturation data of three single-labeled MARCKS (151-175) peptides in PC:PIP_2 is shown in Figure 4.1-21. Table 4.1-3 list the Φ values obtained, the corresponding depth value and the depth value for these peptides previously obtained in PC:PS. For the middle and C-terminal portion of the peptide, the depth of the spin-label is at about 7Å below the lipid phosphate. The spin-label placed at the N-terminus is several Å off of the lipid bilayer in the aqueous phase. Within experimental error, there is no difference in the depth of the MARCKS peptides regardless of whether the vesicles contain PC:PS or PC:PIP_2.

4.2. Discussion

The motivation for the work described here was two-fold. The first goal was to characterize a spin-labeled PIP_2 molecule that could be used to probe the lipid's distribution and interactions within the lipid bilayer. The second goal was to further distinguish the interaction between the MARCKS effector domain and PIP_2.

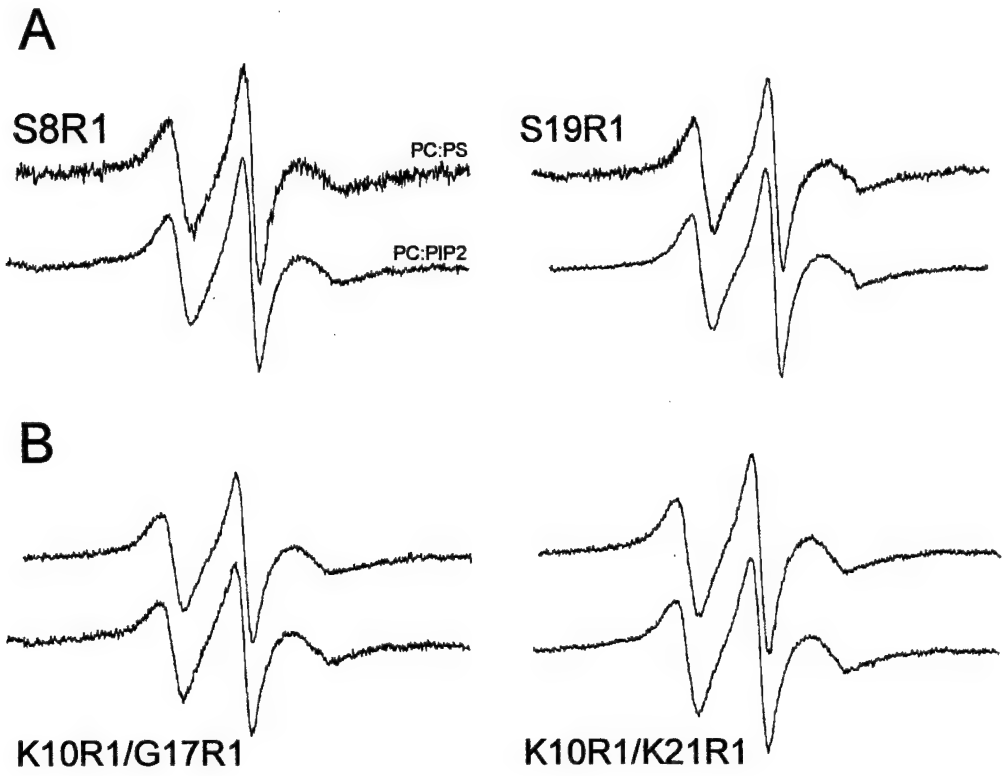

Figure 4.1-20 EPR spectrum of A) single labeled MARCKS peptides S8R1 and S19R1 B) double labeled MARCKS peptides K10R1/G17R1 and K10R1/K21R1 in PC:PS (top spectra) and PC:PIP_2 (bottom spectra)

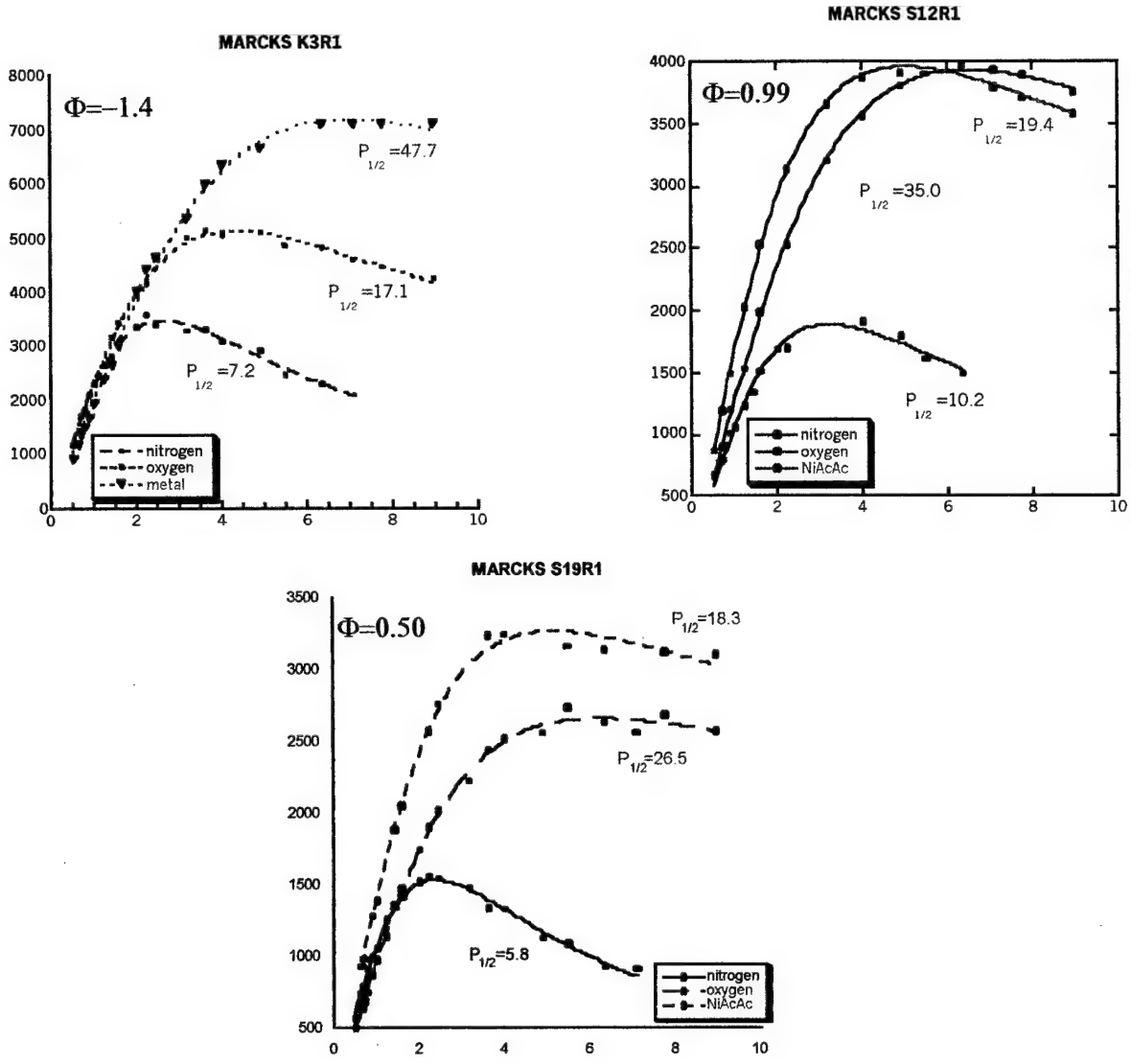

Figure 4.1-20 Power saturation data of K3R1, S12R1 and S19R1 MARCKS (151-175) peptides in 40 mM PC 2% PIP_2 vesicles, 20 mM NiAcAc was used as the polar relaxing agent.

Peptide	Φ (PC:PIP_2)	d (PC:PIP_2)	d (PC:PS)
K3R1	-1.4	-2 Å	-4 Å
S12R1	1.0	+10 Å	+7 Å
S19R1	0.5	+7 Å	+6 Å

Table 4.1-3 Φ values and corresponding depth, d, within the membrane bilayers. PC:PS values were published previously (Qin, 1996). The d value for S19R1 in PC:PS is the average depth obtained for neighbor residues 21 and 22. Error for depth measurements is approximately ±2Å

The proxyl-PIP_2 molecule obtained from Dr. Glenn Prestwich was found to dissolve readily in chloroform and incorporates reproducibly as a monomer into the external surface of lipid vesicles. The EPR spectrum of the proxyl-PIP_2 shows the proxyl-label to have a relatively fast rotational correlation time.

Power saturation of the EPR spectrum of the proxyl-PIP_2 places the proxyl-label location near the membrane interface. If the acyl chain with the proxyl-spin label were fully extended and the PIP_2 head group was situated at the same place in the membrane bilayer as the PC or PS head group, then the proxyl label should reside at a depth of about 15 Å below the lipid phosphate. There are two probable causes for the difference in depth of the spin-label. First, the acyl chain attached to the proxyl label maybe bent at such an angle as to place the label at the membrane interface. Second, the PIP_2 headgroup has a net 3- charge at neutral pH. The negatively charged PS in the vesicles may, through repulsive forces, prohibit the proxyl-PIP_2 headgroup from fully incorporating into the lipid bilayer, causing the proxyl-PIP_2 to sit slightly more into the aqueous phase than the other lipids in the membrane. With the combination of both a bent acyl chain and the negatively charged headgroup it is quite realistic to expect the depth of the proxyl-label to be positioned at the interface of the lipid bilayer.

Upon addition of neomycin and the PLC δ_1 PH domain, two well documented PIP_2 binding molecules, the EPR spectrum broadens. This broadening is indicative of a reduction of spin label motion. The reduction in the motion is caused by a change in the spin label dynamics upon proxyl-PIP_2 binding to either neomycin or the PLC δ_1 PH domain. Initially it is difficult to visualize how the motion of the proxyl spin label attached to the flexible acyl chain should be directly affected by the binding of the

neomycin or the PLC δ_1 PH domain to the charged lipid head group. However, binding of the head group to a larger macromolecule would cause a decrease in the rotational motion of the lipid molecule, thereby decreasing the overall rotational correlation time of the molecule. This decrease in rotational correlation time results in broadening of the spectrum. In addition, if the binding of the molecules to the PIP_2 head group causes a change in location and/or environment of the proxyl-label, this too may cause a broadening in the spectrum. Therefore, it is possible to conclude that both neomycin and the PLC δ_1 PH domain bind strongly to the proxyl-PIP_2 head group and as a consequence slow down the rotational motion of the proxyl-PIP_2 molecule as a whole.

Titration of the EPR spectra with neomycin shows the identical 1:1 stoichemetry found for native PIP_2-neomycin binding interactions. The apparent molar partition coefficient of neomycin for proxyl- PIP_2, 3×10^5 M^{-1}, was also found to be almost identical to the value, 10^5 M^{-1} previously documented (Arbuzova et al., 2000a).

A developing hypothesis for the regulation of accessibility and lateral distribution of PIP_2 is sequestering of the molecule by proteins and binding motifs (Raucher et al., 2000).

A peptide from the sequence of the MARCKS effector domain has recently been shown to bind strongly to multiple PIP_2s (Wang et al., 2001). The MARCKS protein also inhibits the hydrolysis of PIP_2 by PLC. These findings suggest the role for MARCKS shown in Figure 4.2-1, where MARCKS binds to multiple PIP_2s at the membrane interface. The MARCKS-PIP_2 interaction prohibits the PIP_2 from freely diffusing within the membrane bilayer, as well as protecting PIP_2 from PLC. The interaction can be

interrupted by removing MARCKS either through phosphorlyation by PKC or by binding to calmodulin.

The experimental work that has been described here supports the MARCKS-PIP_2 interaction depicted in Figure 4.2-1. The strong interaction of the proxyl-PIP_2 with the MARCKS (151-175) peptide manifests through the broadening of EPR spectrum. In addition, evidence for multiple PIP_2s binding to the peptide exists. Comparison of the proxyl-PIP_2 EPR spectra show increased broadening in the presence of MARCKS compared to in the presence of neomycin or PLC δ_1 PH domain. Upon 3:1 dilution of the proxyl-PIP_2 with unlabeled PIP_2, the EPR spectrum does not show the same broadening in the presence of MARCKS (151-175). The dilution experiment data supports that the increased broadening is caused by spin-spin exchange of close proximity proxyl-PIP_2s. Low temperature EPR spectra of the diluted and undiluted proxyl-PIP_2 further support this conclusion. Finally, titration of the EPR spectrum with MARCKS (151-175) was best fit with a stoicheometry of about 2.5 to 3.5 proxyl-PIP_2 to MARCKS, a value in agreement with the ratio found by electrophoretic mobility measurements (Wang et al., 2001).

The binding of the MARCKS (151-175) peptide to the multiple proxyl-PIP_2s is strong enough to change the dynamics of the proxyl spin-label, either through decreasing the lipid molecule's rotational motion or an environmental constriction on the label or some combination of both. The data obtained from comparing the spin-labeled MARCKS (151-175) cysteine derivative peptides indicate that while binding between the MARCKS peptide and multiple PIP_2 is strong, it does not cause a change in conformation of the peptide. Nor does this strong binding seem to require any specific molecular

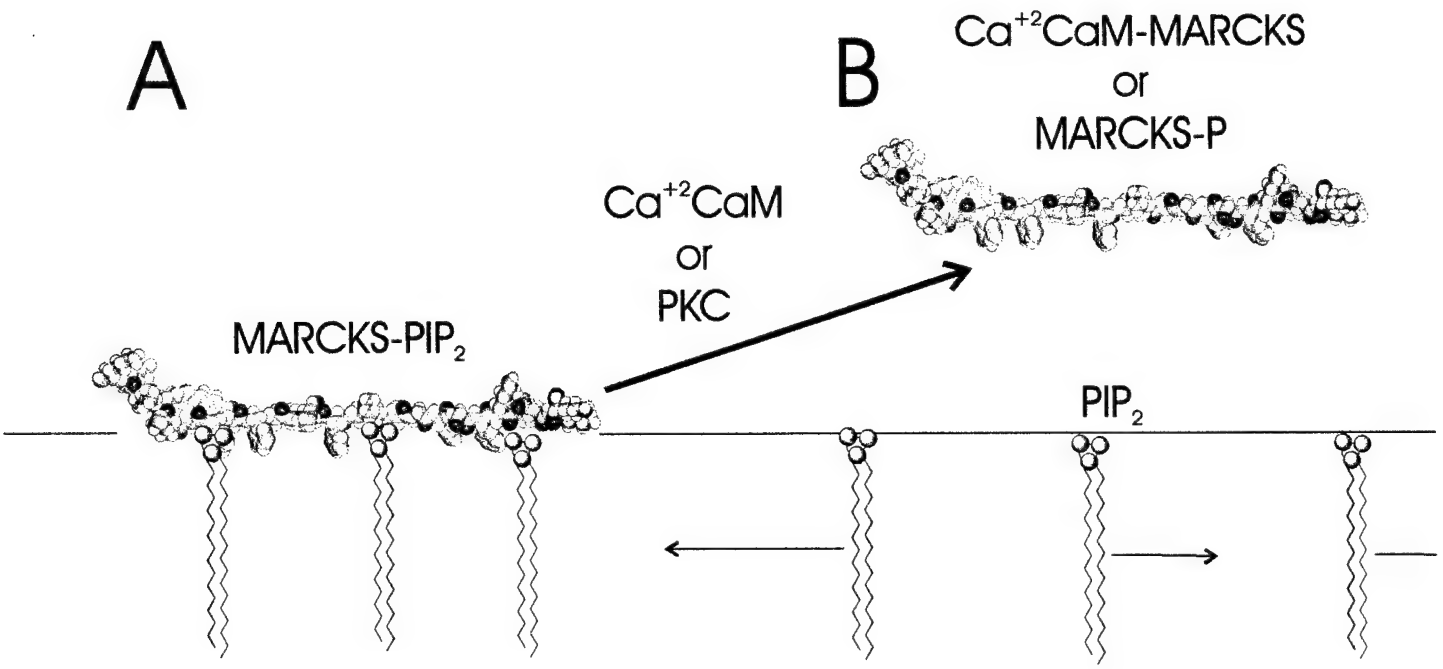

Figure 4.2-1 Depiction of MARCKS effector domain A) regulating PIP_2 through electrostatic motivated binding until B) MARCKS is released from the membrane through binding with Ca+Calmodulin or phosphorylation by PKC thereby allowing PIP_2 to migrate through the plane of the bilayer

conjunction with the first five. All of this evidence supports the hypothesis that the binding of MARCKS and PIP_2 is driven by electrostatic forces.

4.3 Conclusion

In conclusion, a spin-labeled PIP_2 derivative was shown to be a successful probe of PIP_2 and PIP_2 binding molecule interactions. Changes in the dynamics of the proxyl spin label EPR spectrum can indicate interactions at the membrane interface. The proxyl-PIP_2 probe can be used to determine stoicheometry of PIP_2-binding interactions and examination of dipolar broadening can indicate PIP_2 domain formation. The proxyl-PIP_2 was used to investigate the binding of the MARCKS effector domain to PIP_2 and showed a binding of 3:1 lipid to peptide. The MARCKS-PIP_2 interaction was further exploited by utilizing spin-labeled MARCKS (151-175) peptides. The data supported the conclusion that the association is non-specific, causes no conformational changes in the MARCKS and is caused by electrostatic interactions. Finally, all of the evidence presented advocates the hypothesis that MARCKS acts to sequester PIP_2 within the membrane bilayer.

References

Aderem, A. A., K. A. Albert, M. M. Keum, J. K. T. Wang, P. G. Gard, and Z. A. Cohn. 1988. Stimulus-dependent myristoylation of a major substrate for protein kinase C. *Nature.* 332:362-364.

Albert, K. A., S. I. Walaas, J. K. T. Wang, and P. Greengard. 1986. Widespread occurrence of "87 kDa", a major specific substrate fo protein kinase C. *Proceedings of the National Academy of Science.* 83:2822-2826.

Altenbach, C., S. L. Flitsch, H. G. Khorana, and W. L. Hubbell. 1989. Structural Studies on Transmembrane Proteins. 2. Spin Labeling of Bacteriorhodopsin Mutants at Unique Cysteines. *Biochemistry.* 28:7806-7812.

Altenbach, C., D. A. Greenhalgh, H. G. Khorana, and W. L. Hubbell. 1994. A collision gradient method to determine the immersion depth of nitroxides in lipid bilayers: Application to spin-labeled mutants of bacteriorhodopsin. *Proceedings of the National Academy of Sciences United States of America.* 91:1667-1671.

Arbuzova, A., K. Martushova, G. Hangyas-Mihalyne, A. J. Morris, S. Ozaki, G. D. Prestwich, and S. McLaughlin. 2000a. Fluorescently labeled neomycin as a probe of phosphatidylinositol-4,5-bisphosphate in membranes. *Biochimica et Biophysica Acta.* 1464:34-48.

Arbuzova, A., J. Wang, D. Murray, J. Jacob, D. S. Cafiso, and S. McLaughlin. 1997. Kinetics of Interaction of the Myristoylated Alanine-rich C Kinase Substrate, Membranes and Calmodulin. *The Journal of Biological Chemistry.* 272:27167-27177.

Arbuzova, A., L. Wang, J. Wang, G. Hangyas-Mihalyne, D. Murray, B. Honig, and S. McLaughlin. 2000b. Membrane Binding of Peptides Containing Both Basic and Aromatic Residues. Experimental Studies with Peptides Corresponding to the Scaffolding Region of Caveolin and the Effector Region of MARCKS. *Biochemistry.* 39:10330-10339.

Ben-Tal, N., B. Honig, R. M. Peitzsch, G. Denisov, and S. McLaughlinf. 1996. Binding of Small Basic Peptides to Membranes Containing Acidic Lipids: Theoretical Models and Experimental Results. *Biophysical Journal.* 71:561-575.

Blackshear, P. J. 1993. The MARCKS Family of Cellular Protein Kinase C Substrates. *The Journal of Biological Chemistry.* 268:1501-1504.

Brand, S. H., and J. D. Castle. 1993. SCAMP 37, a new marker within the general cell surface recycling system. *The EMBO Journal.* 12:3753-3761.

Brand, S. H., S. M. Laurie, M. B. Mixon, and J. D. Castle. 1991. Secretory Carrier Membrane Proteins 31-35 Define a Common Protein Composition among Secretory Carrier Membranes. *The Journal of Biological Chemistry.* 266:18949-18957.

Bucki, R., F. Giraud, and J.-C. Sulpice. 2000. Phosphatidylinositol 4, 5-Bisphosphate Domian INducers Promote Phospholipid Transverse Redistribution in Biological Membranes. *Biochemistry.* 39:5838-5844.

Chauhan, V. P. S. 1990. Phosphatidylinositol 4, 5-bisphosphate stimulates protein kinase C-mediated phosphorylation of soluble brain proteins. Inhibition by neomycin. *FEBS Letters.* 272:99-102.

Corradin, S., A. Ransijn, G. Corradin, M. A. Roggero, A. A. P. Schmitz, P. Schneider, J. Mauel, and G. Vergeres. 1999. MARCKS-related Protein (MRP) Is a Substrate for the *Leishmania major* Surface Protease Leishmanolysin (gp63). *The Journal of Biological Chemistry.* 274:25411-25418.

Czech, M. P. 2000. PIP2 and PIP3: Complex Roles at the Cell Surface. *Cell.* 100:603-605.

Ferguson, K. M., M. A. Lemmon, J. Schlessinger, and P. B. Sigler. 1994. Crystal Structure at 2.2 A Resolution of the Pleckstrin Homology Domain from Human Dynamin. *Cell.* 79:199-209.

Ferguson, K. M., M. A. Lemmon, J. Schlessinger, and P. B. Sigler. 1995. Structure of the High Affinity Complex of Inositol Triphosphate with a Phospholipase C Pleckstrin Homology Domain. *Cell.* 83:1037-1046.

Fernandez-Chacon, R., G. DeToledo, R. Hammer, and T. Suedhof. 1999. Analysis of SCAMP 1 Function in Secretory Vesicle Exocytosis by means of Gene Targeting in Mice. *Journal of Biological Chemistry.* 274:32551-32554.

Fiske, C. H., and Y. Subbarow. 1925. *Journal of Biological Chemistry.* 66:375.
Gibson, T. J., M. Hyvonen, A. Musacchino, and M. Saraste. 1994. PH domain: the first anniversary. *TIBS.* 19:349-353.

Glaser, M., S. Wanaski, C. A. Buser, V. Boguslavsky, WahidSRashidzada, A. Morris, M. Rebecchi, S. F. Scarlata, L. W. Runnels, G. D. Prestwich, J. Chen, A. Aderem, J. Ahn, and S. McLaughlin. 1996. Myristoylated Alanine-rich C Kinase Substrate (MARCKS) Produces Reversible Inhibition of Phospholipase C by Sequestering Phosphatidylinositol 4,5-Bisphosphate in Lateral Domains. *The Journal of Biological Chemistry.* 271:26187-26193.

Gordon, and Breach. Electron Paramagnetic Resonance.

Gross, A., L. Columbus, K. Hideg, C. Altenbach, and W. L. Hubbell. 1999. Structure of the KcsA Potassium Channel from Streptomyces lividans: A Site-Directed Spin Labeling Study of the Second Transmembrane Segment. *Biochemistry.* 38:10324-10335.

He, M. M., J. Voss, W. L. Hubbell, and H. R. Kaback. 1997. Arginine 302 (Helix IX) in the Lactose Permease of *Escherichia coli* Is in Close Proximity to Glutamate 269 (Helix VIII) as Well as Glutamate 325 (Helix X). *Biochemistry.* 36:13682-13687.

Hirata, M., T. Kanematsu, H. Takeuchi, and H. Yagisawa. 1998. Pleckstrin Homology Domain as an Inositol Compound Binding Module. *Japanese Journal of Pharmacology.* 76:255-263.

Hubbard, C., D. Singleton, M. Rauch, S. Jayasinghe, D. Cafiso, and D. Castle. 2000. The secretory carrier membrane protein family: structure and membrane topology. *Molecular Biology of the Cell.* 11:2933-2937.

Hubbell, W. L., and C. Altenbach. 1994. Investigation of Structure and Dynamics in Membrane Proteins using Site-Directed Spin Labeling. *Current Opinion in Structural Biology.* 4:566-578.

James, G., and E. N. Olson. 1989. Myristoylation, Phosphorylation and Subcellular Distribution of the 80-kDa Protein Kinase C Substrate in BC_3H1 Myocytes. *The Journal of Biological Chemistry.* 264:20928-20933.

Kim, J.-M., C. Altenbach, R. L. Thurmond, H. G. Khorana, and W. L. Hubbell. 1997. Structure and function in rhodopsin: Rhodopsin mutants with a neutral amino acid at E134 have a partially activated conformation in the dark state. *Proceedings of the National Academy of Sciences USA.* 94:14273-14278.

Klug, C. S., W. Su, and J. B. Feix. 1997. Mapping of the Residues Involved in a Proposed B-Strand Located in the Ferric Enterobactin Receptor FepA Using Site-Directed Spin-Labeling. *Biochemistry.* 36:13027-13033.

Lemmon, M. A., K. M. Ferguson, R. O'Brien, P. B. Sigler, and J. Schlessinger. 1999. Specific and high-affinity binding of inositol phosphates to an isolated pleckstrin homology domian. *Proceedings of the National Academy of Sciences of the United States of America.* 92:10472-10476.

Lemmon, M. A., K. M. Ferguson, and J. Schlessinger. 1996. PH Domains: Diverse Sequences with a Common Fold Recruit Signaling Molecules to the Cell Surface. *Cell.* 85:621-624.

Martin, T. F. 1997. Phosphoinositides as spatial regulators of membrane traffic. *Current Opinion in Neurobiology.* 7:331-338.

Mathews, C. K., and K. E. V. Holde. 1996. Biochemistry. The Benjamin/Cummings Publishing Company Inc., Menlo Park.

Mayer, B. J., R. Ren, K. L. Clark, and D. Baltimore. 1993. A Putative Modular Domain Present in Diverse Signaling Proteins. *Cell.* 73:629-630.

Mchaourab, H. S., M. A. Lietzow, K. Hideg, and W. L. Hubbell. 1996. Motion of Spin-Labeled Side Chains in T4 Lysozyme. Correlation with Protein Structure and Dynamics. *Biochemistry.* 35:7692-7704.

Mchaourab, H. S., K. J. Oh, C. J. Fang, and W. L. Hubbell. 1997. Conformation of T4 Lyzozyme in Solution. Hinge-Bending Motion and the Substrate-Induced Conformational Transition
Studied by Site-Directed Spin Labeling. *Biochemistry.* 36:307-316.

Nordio, P. L. 1976. General Magnetic Resonance Theory. *In* Spin-labeling Theory and Applications. L. J. Berliner, editor. Academic Press Inc.f, New York.

Ohmitsu, M., K. Fukunaga, H. Yamamoto, and E. Miyamoto. 1999. Phosphorylation of Myristoylated Alanine-rich Protein Kinase C Substrate by Mitogen-activated Protein Kinase in Cultured Rat Hippocampal Neurons following Stimulation of Glutamate Receptors. *The Journal of Biological Chemistry.* 274:408-417.

Qin, Z., and D. S. Cafiso. 1996. Membrane Structure of Protein Kinase C and Calmodulin Binding Domain of Myristoylated Alanine Rich C Kinase Substrate Determined by Site-Directed Spin Labeling. *Biochemistry.* 35:2917-2925.

Rabenstein, M. D., and Y.-K. Shin. 1995. Determination of the distance between two spin labels attached to a macromolecule. *Proceedings of the National Academy of Science United States of America.* 92:8239-8243.

Raucher, D., T. Stauffer, W. Chen, K. Shen, S. Guo, J. D. York, M. P. Sheetz, and T. Meyer. 2000. Phosphatidylinositol 4,5-Bisphosphate Functions as a Second Messenger that Regulates Cytoskeleton-Plasma Membrane Adhesion. *Cell.* 100:221-228.

Robinson, B., H. Thomann, A. Beth, P. Fajer, and L. Dalton. 1985. The Phenomenon of Magnetic Resonace: Theoretical Considerations. *In* EPR and Advanced EPR Studies of Biological Systems. L. R. Dalton, editor. CRC Press, Inc., Boca Raton. 11-111.

Shaw, G. 1996. The pleckstrin homology domain: an intriguing multifuntional protein module. *Bioessays.* 18:35-46.

Tall, E., G. Dorman, P. Garcia, L. Runnels, S. Shah, J. Chen, A. Profit, Q.-M. Gu, A. Chaudhary, G. Prestwich, and M. J. Rebecchi. 1997. Phosphoinositide Binding Specificity among Phospholipase C Isozymes as Determined by Photo-Cross-Linking to Novel Substrate and Product Analogs. *Biochemistry.* 36:7239-7248.

Taniguchi, H., and S. Manenti. 1993. Interaction of Myristoylated Alanine-rich Protein Kinase C Substrate (MARCKS) with Membrane Phospholipids. *The Journal of Biological Chemistry.* 268:9960-9963.

Toker, A. 1998. The synthesis and cellular roles of phosphatidylinositol 4,5 bisphosphate. *Current Opinion in Cell Biology.* 10:254-261.

Vanhaesebroeck, B., S.J. Leevers, K. Ahmadi, J. Timms, R. Katso, P.C. Driscoll, R. Woscholski, P.J. Parker and M.S. Waterfield. Synthesis and Function of 3-Phosphorylated Inositol Lipids. *Annuals of Biochemistry.* 70:535-602.

Victor, K., J. Jacob, and D. S. Cafiso. 1999. Interactions Controlling the Membrane Binding of Basic Protein Domains: Phenylalanine and the Attachment of the Myristoylated Alanine-Rich C-Kinase Substrate Protein to Interfaces. *Biochemistry.* 38:12527-12536.

Victor, K. G., and D. S. Cafiso. 2001. Location and Dynamics of Basic Peptides at the Membrane Interface: EPR Spectroscopy of TOAC Labeled Peptides. *Biochemistry.* to be published.

Wang, J., A. Arbuzova, G. Hangyas-Mihalyne, and S. McLaughlin. 2001. The Effector Domain of Myristoylated Alanine-rich C Kinase Substrate Binds Strongly to Phosphatidylinositol 4,5-Bisphosphate. *The Journal of Biological Chemistry.* 276:5012-5019.

Wang, J. K. T., S. I. Walaas, T. S. Sihra, A. Aderem, and P. Greengard. 1989. Phosphorylation and associated translocation of the 87-kDa protein, a major protein kinase C substrate, in isolated nerve terminals. *Proceedings of the National Academy of Science.* 86:2253-2256.

Wang, Q., J. Voss, W. L. Hubbell, and H. R. Kaback. 1998. Proximity of Helices VIII (Ala 273) and IX (Met299) in the Lactose Permease of *Escherichia coli. Biochemistry.* 37:4910-4915.

Wu, T. T., and J. D. Castle. 1997. Evidence for colocalization and interaction between 37 and 39 kDa isoforms of secretory carrier membrane proteins (SCAMPs). *Journal of Cell Science.* 110:1533-1541.

Wu, W. C. S., S. I. Walaas, A. C. Nairn, and P. Greengard. 1982. Calcium/phospholipid regulates phosphorylation of a M_r "87k" substrate protein in brain synaptosomes. *Proceedings of the National Academy of Science.* 79:5249-5253.

Yamauchi, E., R. Kiyonami, M. Kanai, and H. Taniguchi. 1998. The C-terminal Conserved Domain of MARCKS Is Phosphorylated *in Vivo* by Proline-directed Protein Kinase. *The Journal of Biological Chemistry.* 273:4367-4371.

Zolessi, F. R., U. Hellman, A. Baz, and C. Arruti. 1999. Characterization of MARCKS (Myristolated Alanine-Rich C Kinase Substrate) Identified by a Monoclonal Antibody Generated against Chick Embryo Neural Retina. *Biochemical and Biophysical Research Communications.* 257:480-487.